

THERMODYNAMIC PROPERTIES OF THE SOLID SOLUTIONS
OF KI-KBr AND OF NH₄I-KI

by

Robert Weintraub, A.B.

Hunter College of the
City University of New York
(1971)

SUBMITTED IN PARTIAL FULFILLMENT

OF THE REQUIREMENTS FOR THE

DEGREE OF DOCTOR OF

PHILOSOPHY

AT THE

MASSACHUSETTS INSTITUTE OF

TECHNOLOGY

August, 1974

Signature redacted

Signature of Author Department of Chemistry

Signature redacted

Certified by Thesis Supervisor

Signature redacted

Accepted by Chairman, Departmental Committee
on Graduate Students

Archives



This Doctoral Thesis has been examined by a committee of the
Department of Chemistry as follows:

Signature redacted

Chairman: Prof. C. Garland

Signature redacted

Thesis Supervisor: Prof. C. Stephenson

Signature redacted

Prof. R. Lord

THERMODYNAMIC PROPERTIES OF THE SOLID SOLUTIONS
OF KI-KBr AND OF NH₄I-KI

by

Robert Weintraub, A.B.

Submitted to the Department of Chemistry
on August 12, 1974 in partial fulfillment of the
requirements for the degree of Doctor of Philosophy

ABSTRACT

An experimental study of the equilibrium compositions in the three-component system KI-KBr-H₂O at 298°K and at 367°K, and of the three-component system NH₄I-KI-H₂O, is reported. The existence of a metastable region of homogeneous solid solutions in the three-component KI-KBr-H₂O system at 298°K is shown.

From these results, the free energy of mixing for the two-component system of solid solutions of KI-KBr is calculated and expressed as a function of temperature and composition by the following equation:

$$\Delta G = RT(X_1 \ln X_1 + X_2 \ln X_2) + RTX_1 X_2 [B_g + C_g (X_1 - X_2)],$$

$$\text{where } B_g = 824.08/T - .2995, \text{ and } C_g = -44.87/T.$$

The thermodynamic quantities calculated from the above expression for the KI-KBr system are consistent with the experimental data obtained in the present study at 298°K and at 367°K, and with other data for the enthalpy of mixing and the solidus-liquidus curves. The range of validity of this expression is about 1000°.

The free energy of mixing for the two-component system NH₄I-KI at 298°K is given by the following equation:

$$\Delta G = RT(X_1 \ln X_1 + X_2 \ln X_2) + RTX_1 X_2 [.400 - .020(X_1 - X_2)].$$

The deviation from an ideal free energy of mixing for this system is smaller than that of any other two-component alkali metal halide system.

Thesis Supervisor: Clark C. Stephenson
Title: Professor of Chemistry

ACKNOWLEDGEMENTS

This work was conducted with the help, guidance, equipment and financial aid of many different individuals and groups of individuals. I take this page to thank some of these people.

I thank Professor C. Stephenson for allowing me the opportunity to work with him. He was intimately involved with this work in all of its stages. He taught, by example, an appreciation of scientific research both in and out of the laboratory.

I thank Professor C. Garland and Professor R. Lord for the continual interest they have shown in this work. Their presence on my Thesis Committee is appreciated.

I thank Professor J. Ross for partial support during the Fall term, 1973, and for giving me an opportunity to learn about an area of research outside that of my thesis work.

I thank the Chemistry Department for giving me the opportunity, while a teaching assistant and while working with course development, to meet the many individuals who were students in the courses I assisted with. I have learned much of value from these individuals.

I thank Mr. E. Curtis for his continual help in making equipment available for my use. I thank Professor R. Lagow for allowing me to spend many hours reading x-ray films in his lab. I thank Dr. M. Laprade for use of her Powder camera and also for several helpful discussions concerning powder techniques. I thank Dr. K. R. Chien for many interesting discussions concerning experiments. I thank Mr. H. Garber, with whom I have had the good fortune to share apartments with these last three years, for many avid midnight chemistry discussions.

I thank my parents and family for their continual encouragement. I also thank many good friends for encouragement.

I am grateful to Ms. Carol Johnson and Ms. Joanne Klotz for their efforts in typing this thesis; they did fine work.

Bruno, the dog, is also thanked for the many interesting walks he took me on.

TABLE OF CONTENTS

	<u>Page</u>
Title Page	1
Examination Page	2
Abstract	3
Acknowledgements	4
Table of Contents	6
List of Figures	10
List of Tables	11
I. Introduction	13
II. Experimental	24
A. Description of Chemicals and Equipment Used in Preparing Complexes	24
1. Chemicals Used to Form Complexes	24
2. Constant Temperature Bath at 25°C	24
3. Constant Temperature Bath and Solution Vessels at 100°C	24
4. Solution Vessels and Stirring Devices at 25°C	25
B. Preparation of Three-Component Complexes	26
1. Stable Equilibrium System KI-KBr-H ₂ O at 25°C	26
a. Near-Duplicate Complexes of Arbitrary Composition	26
i. Preparation of Saturated Liquid Solution from Oversaturation	26
ii. Preparation of Near-Duplicate Complexes	27
b. Near-Duplicate Complexes by the Method of the Infinitesimal Approach to the Limiting Miscibility	27

	<u>Page</u>
i. Procedure	27
ii. Method of Preparation of the Isothermally Invariant Liquid Solution When the Composition is Unknown	27
iii. Method of Preparation of the Isothermally Invariant Liquid Solution When the Composition is Known	29
2. Metastable Equilibrium by the Method of Isothermal Relief of Supersaturation in the System KI-KBr-H ₂ O at 25°C	29
3. KI-KBr-H ₂ O at 94°C by the Method of Isothermal Evaporation	30
4. KI-NH ₄ I-Third-Component at 25°C by the Method of Duplicate Complexes	31
C. Chemical Analysis	33
1. System KI-KBr-H ₂ O at 25°C	33
a. Analysis of Liquid Phase	33
i. Weight Per Cent Salt in Liquid Phase	33
ii. Analysis for Br ⁻ in Presence of I ⁻ in Liquid Phase	34
b. Analysis of Solid Phase and Wet Residue	36
i. Weight Per Cent Salt in Solid Phase and Wet Residue	36
ii. Analysis of Br ⁻ in Presence of I ⁻ in Solid Phase and Wet Residue	36
2. System KI-NH ₄ I-Third-Component at 25°C	37
D. X-ray Analysis	37
1. Powder Equipment and Sample Handling	37

	<u>Page</u>
2. X-ray Analysis of the System KI-KBr at 94°C and of NH ₄ I-KI System at 25°C	38
III. Data Analysis and Results	40
A. KI-KBr-H ₂ O at 25°C	40
1. Analytical Method	40
a. Gravimetric Analysis	40
b. Weight Per Cent Salt	45
2. Results of Analyses	45
B. KI-KBr-H ₂ O at 94°C	59
1. Analytical Method	59
2. Results of Analyses	63
C. KI-NH ₄ I-Third-Component at 25°C	67
1. Analytical Method	67
2. Results of Analyses	67
IV Discussion	76
A. KI-KBr and KI-KBr-H ₂ O at 25°C	76
B. KI-KBr at All Temperatures and KI-KBr-H ₂ O at 94°C	91
C. NH ₄ I-KI and NH ₄ I-KI-H ₂ O at 25°C	103
D. Conclusions	108
Appendix I Approximations for the Strictly Regular and Symmetrical Solution	115
Appendix II Powder Pattern Data	116
Appendix III KI-KBr-H ₂ O at 25°C, Calculated Using $\log \frac{\gamma_1^2}{\gamma_2} = \text{function of } m_1 \text{ and } m_2$ Employing Equations (4.11) and (4.12) Valid only in Range of Experimental Data for Total Molalities	140

	<u>Page</u>	
Appendix IV	KI-KBr-H ₂ O at 25°C, Calculated for Whole Range of Mole Fractions in Aqueous Liquid Phase and Solid Phase Assuming $\log \frac{\gamma_1^2}{\gamma_2} = \text{constant}$	142
Appendix V	Free Energy of Mixing for the KI-KBr System at 298.15°K, 361.08°K (the Critical Mixing Temperature) and at 400.00°K	143
Appendix VI	Activities of KI and KBr in Solid Phase at 298°K	144
Appendix VII	KI-KBr-H ₂ O at T = 367°K, Calculated Mole Fractions Dissolved Salts in Aqueous Phase and Solid Phase	145
Appendix VIII	KI-KBr, ΔH^M and ΔS^M	146
Appendix IX	KI-KBr, Calculated Solvus Curve	147
Appendix X	Liquidus-Solidus Curves Calculated	148
Appendix XI	NH ₄ I-KI-H ₂ O at 298°K, Mole Fraction X_1^S and X_1^L Calculated	149
Appendix XII	NH ₄ I-KI at 298°K, Free Energy of Mixing	150
References		151
Biographical Note		153

LIST OF FIGURES

<u>Figure No.</u>	<u>Title</u>	<u>Page</u>
1.	KI-KBr-H ₂ O at 298.15°K, Log D Versus Mole Fraction KI Solid Phase, Experimental and Calculated	110
2.	KI-KBr-H ₂ O at 367°K, Log D Versus Mole Fraction KI, Experimental and Calculated	111
3.	Free Energy of Mixing of Solid Solutions of KI-KBr Below the Critical Mixing Temperature, at the Critical Mixing Temperature, and Above the Critical Mixing Temperature	112
4.	KI-KBr, Liquidus and Solidus Curves, Calculated and Experimental	113
5.	NH ₄ I-KI-H ₂ O at 298.15°K, Log D Versus Mole Fraction, Experimental and Calculated	114

LIST OF TABLES

<u>Table No.</u>	<u>Title</u>	<u>Page</u>
II (1)	Chemicals Used in Analysis for Br ⁻ in the Presence of I ⁻	35
III (1)	Analysis of Known Samples of Mixtures of KI and KBr	42
III (2)	Weight Per Cent Salt and Molality in Saturated Water Solution at 25°C for Pure Components KI and KBr	46
III (3)	Experimental Results for KI-KBr-H ₂ O at 25°C	48
III (4)	KI-KBr-H ₂ O at 25°C, Mole Per Cent Dissolved Salts and Solid Phase: Equilibrium Data	52
III (5)	KI-KBr-H ₂ O at 25°C, Mole Per Cent Dissolved Salts and Solid Phase: Metastable Equilibrium	53
III (6)	KI-KBr-H ₂ O at 25°C, Mole Per Cent Dissolved Salts and Solid Phase: Non-Equilibrium	54
III (7)	Sample Calculation: Mass Balance for Complexes D and E	55
III (8)	Lattice Parameters at Room Temperature for Pure Components KI and KBr	60
III (9)	Calibration of x-ray Data	61
III (10)	Mole Per Cent Dissolved Salts, Composition of Solid Phase, and Lattice Parameter (x-rayed at Room Temperature) for KI-KBr-H ₂ O at 94°C	64
III (11)	Experimental Results for NH ₄ I-KI-H ₂ O at 25°C	68
III (12)	NH ₄ I-KI-H ₂ O in Weight Per Cent	70
III (13)	NH ₄ -KI-H ₂ O in Mole Per Cent	71
III (14)	Lattice Parameters at Room Temperature for Pure Components and Solid Solutions of KI-NH ₄ I	74
III (15)	Solubility Determination of Pure NH ₄ I at 25°C	75

LIST OF TABLES

<u>Table No.</u>	<u>Title</u>	<u>Page</u>
IV (1)	KI-KBr-H ₂ O at 25°C, Experimental Values of Activity Coefficients in Liquid and Solid Phases (parts a and b)	80
IV (2)	KI-KBr-H ₂ O at 25°C, log γ_2 : Experimental and Calculated Values	83
IV (3)	KI-KBr-H ₂ O at 25°C, log γ_1 : Experimental and Calculated Values	84
IV (4)	KI-KBr-H ₂ O at 25°C, Experimental and Calculated Molalities of KI	86
IV (5)	KI-KBr-H ₂ O at 25°C, Experimental and Calculated Molalities of KBr	87
IV (6)	KI-KBr-H ₂ O at 25°C, Experimental and Calculated Weight Per Cent Salts in Saturated Solution	88
IV (7)	KI-KBr-H ₂ O at 25°C, Experimental and Calculated Mole Fractions of Dissolved Salts in Aqueous Phase: Calculated by Two Methods	90
IV (8)	KI-KBr-H ₂ O at 367°K, Experimental and Calculated Mole Fractions of Dissolved Salts in Aqueous Liquid Phase	98
IV (9)	ΔH^M : Experimental Obtained by Koski and Calculated in Present Study	101
IV (10)	NH ₄ I-KI-H ₂ O at 25°C, Experimental Activity Coefficients in Aqueous Liquid and Solid Phases.	105
IV (11)	NH ₄ I-KI-H ₂ O at 25°C, Experimental and Calculated Mole Fractions of Dissolved Salts in Aqueous Liquid Phase	106

CHAPTER I INTRODUCTION

A "solid solution" is a solution existing in the solid state of aggregation. A "solution" is defined as a phase "consisting of a physically homogeneous mixture of two or more substances."¹ A "phase" is "that part of a system that is of uniform structure throughout its entire mass both in chemical composition and physical state."¹ These definitions are given to emphasize the fact that a solid solution is a solution in the rigorous thermodynamic sense.

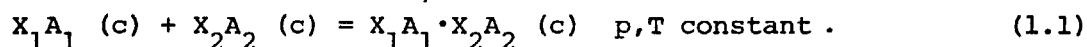
The application of thermodynamics to any system enables the prediction of bulk properties of the system under an unlimited variety of conditions. For these predictions to be sound, a knowledge only of the behavior of these properties under a carefully chosen limited range of conditions is required. This fact has been exploited to a large extent in application to gaseous and liquid solutions. It at first seems surprising that up until the present time few careful studies have involved equilibrium thermodynamics applied to solutions of ionic crystals. This can be explained by the fact that the attainment of equilibrium between solids by its very nature demands that accurate experimental data will be more difficult to obtain than for fluids. It is this difficulty associated with the attainment of equilibrium in solid solutions that is primarily responsible for the lack of quality data in the literature.

The alkali and ammonium halides exhibit much diversity in their behavior in solid solution formation. This fact, along with their simple crystal structures, make them excellent systems to exemplify solid solution behavior in general.

The relationships useful for the evaluation of the thermodynamic

properties of solid solutions will now be presented. The general form of the expressions for the thermodynamic excess of mixing functions that are employed is attributable to Scatchard, Hamer and coworkers.²

The change in state to be considered for the formation of one mole of a two-component solid solution at constant T and p is the following:



X_1 and X_2 represent the mole fraction of components A_1 and A_2 present in the condensed state (c). The free energy change associated with this change in state is termed the "free energy of mixing." The free energy of mixing, ΔG^M , is conveniently represented in the following form:

$$\Delta G^M = \Delta G^{ID} + \Delta G^{XS} , \quad (1.2)$$

where the ideal free energy of mixing is given by

$$\Delta G^{ID} = RT(X_1 \ln X_1 + X_2 \ln X_2) , \quad (1.3a)$$

and the excess free energy of mixing is given by

$$\Delta G^{XS} = RTX_1 X_2 [B_g + C_g(X_1 - X_2) + \dots] , \quad (1.3b)$$

and $B_g = B_h/T - B_s$, (1.4)

and $C_g = C_h/T - C_s$. (1.5)

The subscripts used to label the B and C parameters denote the dependence of each of the parameters on the thermodynamic state functions as shown: g - free energy; s - entropy; h - enthalpy.

The thermodynamic properties shown below are obtained by differentiation of the above equations:

$$\Delta S^{ID} = -R(X_1 \ln X_1 + X_2 \ln X_2) , \quad (1.6a)$$

$$\Delta S^{XS} = +RX_1 X_2 [B_s + C_s(X_1 - X_2) + \dots] , \quad (1.6b)$$

$$\Delta H^{ID} = 0 \quad , \quad (1.7a)$$

$$\Delta H^{XS} = \Delta H^M = RX_1X_2[B_h + C_h(X_1 - X_2) + \dots] \quad , \quad (1.7b)$$

$$\Delta C_{p,x} = 0 \quad , \quad (1.8)$$

$$\bar{G}_1 - G_1^O = RT \ln X_1 + RTX_2^2[B_g + C_g(4X_1 - 1) + \dots] \quad , \quad (1.9)$$

$$\bar{G}_2 - G_2^O = RT \ln X_2 + RTX_1^2[B_g + C_g(4X_1 - 3) + \dots] \quad , \quad (1.10)$$

$$\bar{H}_1 - H_1^O = RX_2^2[B_h + C_h(4X_1 - 1) + \dots] \quad , \quad (1.11)$$

$$\bar{H}_2 - H_2^O = RX_1^2[B_h + C_h(4X_1 - 3) + \dots] \quad . \quad (1.12)$$

Employing the rational system for activity coefficients, pure A_1 and A_2 are selected as the standard and reference states. The following equations are then valid:

$$a_1 = f_1X_1 \quad , \quad (1.13)$$

$$a_2 = f_2X_2 \quad , \quad (1.14)$$

$$\ln f_1 = X_2^2[B_g + C_g(4X_1 - 1) + \dots] \quad , \quad (1.15)$$

$$\ln f_2 = X_1^2[B_g + C_g(4X_1 - 3) + \dots] \quad , \quad (1.16)$$

$$\Delta G^{XS} = X_1RT \ln f_1 + X_2RT \ln f_2 \quad . \quad (1.17)$$

In the above equations, a_1 and a_2 are the activities and f_1 and f_2 are the activity coefficients expressed in terms of mole fractions for components A_1 and A_2 respectively.

The discussion in this thesis employs the terms involving the B and C parameters in equations (2) through (17), with higher order terms neglected. This approximation has been discussed by other workers³ and is shown to be valid by the results of the present study. It has been shown that the approximations used in equations (4) and (5), which lead to the result shown by equation (8), is valid within the limits

of error of the data generally available. The approximations of these equations for the solution which is both strictly regular and symmetrical are given in Appendix I.

All of the thermodynamic values expressed by equations (2) through (17) are known explicitly when the temperature dependent parameters B_g and C_g have been evaluated.

Numerous techniques can be employed to determine the values B_g , B_h , B_s and C_g , C_h and C_s . The parameters with the subscript h can be evaluated directly from ΔH data by employing equation (7). Parameters with the subscript s are related to the ΔS^{XS} and can be evaluated from equation (6).

The parameters with the subscript g are of concern in the present case. These can be evaluated by a combination of ΔH and ΔS data. More direct methods exist, however, which yield B_g and C_g parameters of greater accuracy than the combination methods. Discussed in detail is the application of two of these methods involving two different thermodynamic paths. The free energy of mixing is a state variable, a fact which requires that it have a numerical value that does not depend upon the path by which it has been determined. To verify the experimentally determined free energies of mixing, both of these paths should, if possible, be applied to the same change in state. If the same value of the free energy of mixing is not obtained within the limits of the experimental error from both paths, the data must be considered inconsistent.

In systems containing a miscibility gap that can be determined experimentally, a powerful method exists for evaluating B_g and C_g . This method utilizes the equilibrium that exists between the two solid phases. Consider at constant temperature T and pressure p the following

two equilibria for components A_1 and A_2 in solid solutions α and β .

$$A_1 \text{ (in solid solution } \alpha) = A_1 \text{ (in solid solution } \beta) \quad , \quad (1.18)$$

$$A_2 \text{ (in solid solution } \alpha) = A_2 \text{ (in solid solution } \beta) \quad . \quad (1.19)$$

The two corresponding equilibrium constants are given below:

$$K_{A_1} = \frac{f_1^\beta X_1^\beta}{f_1^\alpha X_1^\alpha} \quad , \quad K_{A_2} = \frac{f_2^\beta X_2^\beta}{f_2^\alpha X_2^\alpha} \quad . \quad (1.20, 21)$$

Here, the mole fractions are those of the limiting miscibility at the temperature T . Recall that

$$\Delta G^0 = -RT \ln K \quad , \quad (1.22)$$

and that here $K = 1$. Take the logarithm of equations (20) and (21)

to obtain the following:

$$0 = \ln f_1^\beta - \ln f_1^\alpha + \ln \frac{X_1^\beta}{X_1^\alpha} \quad , \quad (1.23)$$

$$0 = \ln f_2^\beta - \ln f_2^\alpha + \ln \frac{X_2^\beta}{X_2^\alpha} \quad . \quad (1.24)$$

Substitution of equation (15) into equation (23) and equation (16)

into equation (24) yields the following useful relations:

$$(X_2^\beta)^2 [B_g + C_g(4X_1^\beta - 1)] - (X_2^\alpha)^2 [B_g + C_g(4X_1^\alpha - 1)] + \ln \frac{X_1^\beta}{X_1^\alpha} = 0 \quad , \quad (1.25)$$

$$(X_1^\beta)^2 [B_g + C_g(4X_1^\beta - 3)] - (X_1^\alpha)^2 [B_g + C_g(4X_1^\alpha - 3)] + \ln \frac{X_2^\beta}{X_2^\alpha} = 0 \quad . \quad (1.26)$$

These equations can be used to evaluate the parameters B_g and C_g .

Thus, at any temperature below the critical mixing temperature, only

the limits of the solid-solid miscibility need be known experimentally

to determine the free energy of mixing at that temperature for all mole fractions of the two solids. Further, if the solvus curve, which is the limits of the solid-solid miscibility, is known as a function of temperature, the parameters B_g , B_h , and B_s and C_g , C_h , C_s can then be evaluated by use of equations (4) and (5). Conversely, if these parameters have been determined, the solvus curve can then be calculated and the value of the entropy, enthalpy, and free energy of mixing at any temperature and composition can be evaluated.

At the critical mixing temperature, the second and third derivatives of the free energy of mixing with respect to composition are zero. This leads to the following equations at the critical mixing temperature:

$$B_g(T_c) = \frac{6x_1 - 6x_1^2 - 1}{4x_1^2(1 - x_1)^2}, \quad (1.27)$$

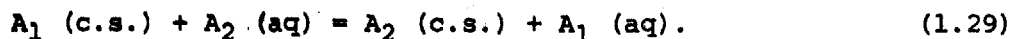
$$C_g(T_c) = -\frac{1 - 2x_1}{12x_1^2(1 - x_1)^2}. \quad (1.28)$$

Thus, if the critical mixing composition is known, the values of B_g and C_g can be determined at the critical mixing temperature. Of more use, however, is the fact that the critical composition and temperature which are generally difficult to determine experimentally can be predicted from the value of B_h , B_s , C_h and C_s determined at lower temperatures.

The equilibrium between two solid phases alone is experimentally very difficult to achieve. A useful technique often employed to aid in the attainment of equilibrium between solid phases is known as the method of the third component. Here, a liquid component is introduced to provide an added medium through which the solids can move. The added liquid also provides an equilibrium by which the free energy of mixing of the two solids can be determined by an independent path.

The added component is usually taken to be water, but this need not necessarily be the case.

Represent the equilibrium between a solid solution and an aqueous phase by the following change in state:



The equilibrium constant for this change in state is given by the following in terms of activities:

$$K = \frac{a_1 \text{ (aq)} a_2 \text{ (c.s.)}}{a_2 \text{ (aq)} a_1 \text{ (c.s.)}} \quad (1.30)$$

The abbreviation "c.s." represents "in an infinite amount of crystalline solid solution of composition $X_1A_1 \cdot X_2A_2$." The abbreviation "aq" represents "dissolved in an aqueous phase." Putting in activity coefficients, the following is obtained when A_1 and A_2 contain a common ion:

$$K = \frac{\gamma_1^2 m_1 (m_1 + m_2) f_2 X_2}{\gamma_2^2 m_2 (m_1 + m_2) f_1 X_1} \quad (1.31)$$

where m_1 and m_2 represent molalities of A_1 and A_2 in the aqueous phase, and the mean activity coefficients γ_1 and γ_2 are those of the components A_1 and A_2 in the three-component aqueous phase. Rearranging and making the following substitution,

$$D = \frac{m_1 X_2 \text{ (c.s.)}}{m_2 X_1 \text{ (c.s.)}} \quad (1.32)$$

the following is obtained:

$$\log K = \log D + \log \frac{\gamma_1^2}{\gamma_2} + \log \frac{f_2}{f_1} \quad (1.33)$$

K is the ratio of the solubility product of A_1 and A_2 . D is called the distribution ratio and can be determined experimentally. Notice that

D can also be expressed by the following:

$$D = \frac{X_1 \text{ (aq)} X_2 \text{ (c.s.)}}{X_2 \text{ (aq)} X_1 \text{ (c.s.)}} \quad (1.34)$$

The term involving the ratio of the activity coefficients γ_1 and γ_2 is generally close to a constant for the saturated three-component aqueous phase. As will be seen in a later section, this term approximates a constant if the total molality change for the series of saturated three-component solutions is small. It is shown later that the experimental data are reproduced within the limits of the experimental error with this approximation introduced.

The ratio of the activity coefficients f_1 and f_2 in the solid phase is given by the following:

$$\ln f_2/f_1 = B_g(2X_1 - 1) + C_g(6X_1^2 - 6X_1 + 1). \quad (1.35)$$

The derivative of equation (33) with respect to mole fraction in the solid phase using the assumption that the ratio of the activity coefficients in the liquid phase is a constant is shown below:

$$2.303 \frac{\partial \log D}{\partial X_1} = -2B_g + 6C_g - 12C_g X_1 \quad (1.36)$$

Thus, the values of B_g and C_g at a temperature T can be obtained from a plot of $\log D$ versus X_1 . In order to determine the B and C terms, the following equations are useful:

$$\frac{\partial \log D_{.50}}{\partial X_1} = \frac{-2B_g}{2.303} = \frac{\log D_{.21} - \log D_{.79}}{.21 - .79} \quad (1.37)$$

$$\log K - \log \frac{\gamma_1^2}{\gamma_2} = 1/2(\log D_{.21} + \log D_{.79}) \quad (1.38)$$

$$C_g/4.606 = \log D_{.50} - 1/2(\log D_{.21} + \log D_{.79}) \quad (1.39)$$

Two thermodynamically independent paths thus exist from which the

free energy parameters B_G and C_G can be evaluated. One path involves only the equilibrium between two solid phases. The other path utilizes the equilibria present in a three-component system. Each path has applications under certain sets of experimental conditions. Equations (25) and (26) can be used to evaluate B_G and C_G in the temperature range below the critical mixing temperature. In the temperature range above the critical mixing temperature, B_G and C_G can more readily be evaluated from equations (33) to (39). At a temperature where the two solids are miscible in all proportions, $\log D$ can be found for all values of X_1 .

The systems lending themselves to the fullest interpretation of the data are those that, at the temperature of study, contain both a miscibility gap and a region of miscibility of the two solids large enough to study the variation of $\log D$ with X_1 . In these cases, B_G and C_G can be evaluated by the two independent paths and the agreement checked for self-consistency of the data.

The systems studied in the present work, KI-KBr and $\text{NH}_4\text{I-KI}$, exemplify some of the diversity seen in ionic crystal solid solution behavior. For studies of this type to be of thermodynamic significance, two experimental criteria must be met. First, the attainment of equilibrium must be demonstrated. Second, the composition of the phases in equilibrium with each other must be determined to sufficient accuracy to enable the free energy parameters to be calculated within useful limits of experimental error.

The KI-KBr system at 298°K contains both a miscibility gap and a large enough region of solid-solid miscibility to study the variation of $\log D$ with mole fraction. This enables the thermodynamic self-consistency of the data to be demonstrated by the two independent paths discussed

earlier in this section. The attainment of equilibrium is demonstrated by approaching equilibrium from two different directions and the data points are shown to lie on the same log D curve regardless of the direction from which the complexes were prepared. The chemical analysis developed for this system has been tested on numerous known samples. The experimental accuracy is shown to be excellent.

The existence of a one-phase region of metastable solid solutions in the three-component system extending into the miscibility gap is demonstrated. The thermodynamic analysis, the method of preparation of these metastable complexes and the agreement between chemical and x-ray analysis each confirm the existence of this region.

The KI-KBr system at 367°K exhibits complete solid-solid miscibility in all proportions. This system is shown to have large deviations from an ideal free energy of mixing and is within 6° of the critical temperature for the appearance of a solid-solid phase separation. The analysis of the composition of the solid phase is by x-ray powder patterns which are calibrated with x-ray photographs of solid solutions of known compositions.

The system $\text{NH}_4\text{I-KI}$ at 298°K exhibits complete miscibility in all proportions. The deviation of this system from an ideal free energy of mixing is shown to be small. Equilibrium is demonstrated by an approach from two directions. The accuracy of the chemical analysis is shown to be excellent.

The free energy of mixing for both of these systems is represented by equation (1.3) using the parameters shown by (1.4) and (1.5). The three parameters derived are sufficient to represent the free energy of mixing for the KI-KBr solid solutions over a range of about 1000°. These parameters are shown to be consistent with the experimental data

obtained in the present study at 298°K and at 367°K, the heats of mixing, and the liquidus-solidus phase equilibrium.

The thermodynamic properties of the $\text{NH}_4\text{I-KI}$ solid solutions at 298°K obtained in the present study are the only relevant data available for this system; consequently, temperature dependence of the free energy cannot be derived. However, because of the small deviation at 298°K from an ideal free energy of mixing, the thermodynamic properties of this system are predicted using the approximation that the system behaves as a strictly regular and symmetrical solution (see Appendix I.)

CHAPTER II. EXPERIMENTAL

A. Description of chemicals and equipment used in preparing complexes

1. Chemicals used to form complexes

The name of the supplier and the grade of each of the chemicals used in the study to form complexes is given below:

Potassium Bromide was of reagent grade supplied by Merck and Co. and conformed to "A. C. S. specifications." Potassium Iodide was of "Baker Analyzed Reagent" grade supplied by the J. T. Baker Chemical Co. Ammonium Iodide was "Certified A. C. S." from Fisher Scientific Co. and "Analytical Reagent" grade supplied by Mallinckrodt Chemical Co.

The NH_4I was dried between 85 and 90°C for six to eight hours before it was used. The KI and KBr were dried above 100°C for two to three hours before use. These salts were used without further purification unless otherwise specified.

The distilled water was supplied by the M. I. T. Physical Plant and was tested for the absence of dissolved chloride by the addition of AgNO_3 and observing no cloudiness.

2. Constant temperature bath at 25°C

A constant temperature bath was maintained at $25.0 \pm .1^\circ\text{C}$. A water pump kept the water in the bath in continuous circulation throughout the bath.

A thermoregulator was set and left at its original setting throughout the course of the experiments. A heating element was controlled by the thermoregulator through a transistorized relay. Cooling tap water flowed into the bath at all times and flowed out constantly through an overflow drain.

3. Constant temperature bath and solution vessels at 100°C

The constant temperature bath at 100°C was a 500 ml beaker containing

boiling water and several boiling chips. The beaker rested on a hotplate to insure continuous boiling. Boiling water was added from time to time to replace water lost by evaporation.

A 250 ml beaker was placed in the water bath and clamped right-side up into place. This beaker held the solution that was to be isothermally evaporated to obtain crystals. The beaker had a thermometer inserted to observe the temperature of the solution. The beaker was kept covered with a Pyrex brand watch glass.

Care was always taken to ensure that the boiling water level in the outer beaker was always higher than the level of the solution in the inner beaker.

4. Solution vessels and stirring devices at 25°C

Erlenmeyer flasks of 1000 ml volume were of either Pyrex or Kimax brand with ground glass stoppers. In experiments where a marble was used, the latter brand was preferred because the bottom of the flasks were slightly concave on the inside which facilitated constant contact between the magnetic stirring bar and the marble.

Air driven stirrers were supplied by the G. Frederick Smith Company. The stirrer was attached to the bottom of the flask by means of rubber bands suspended from the neck of the flask. Metal clamps holding the stirrers in place were used initially but were found to interfere with the stirring. A magnetic teflon brand coated stirring bar was placed inside the erlenmeyer flasks when stirring was desired. Where grinding of the solid phase was desired, a glass marble was also placed inside the erlenmeyer flask. The marble in the flask was constantly rolling around the bottom of the flask being kept in motion by contact with the stirring bar.

The stirrers were powered either by forced air or vacuum.

Flasks placed in the constant temperature bath were shielded from direct light by several layers of paper.

In experiments involving duplicate or near-duplicate complexes, a sheet of rubber was wrapped around the ground glass seal of the erlenmeyer flask to minimize loss of moisture and exchange of gases with the surroundings.

B. Preparation of three component complexes

1. Stable Equilibrium System KI-KBr-H₂O at 25°C

a. Near duplicate complexes of arbitrary composition

i. Preparation of saturated liquid solution from
oversaturation

KI and KBr were each weighed to the nearest .5 grams in various mole ratios. The two solids were placed in a 1000 ml. erlenmeyer flask. Added to this flask was distilled water that had been boiled vigorously for ten to fifteen minutes just prior to its use in order to drive off dissolved gases. The amount of water added was such that at 25°C approximately 20 to 40 grams of the salts would remain in the solid phase. The total volume of these mixtures ranged from 500 to 900 ml.

The open flask was gently warmed on a hotplate with constant agitation until all of the solid had dissolved into the liquid phase. A magnetic stirring bar was then added to the flask and the flask was stoppered with the ground glass top.

The flask was then placed into a constant temperature bath at 25°C. The stirrers were turned on and the flasks were left undisturbed for two to three days. A five ml portion of the liquid solution was pipetted off for analysis.

The bulk of the solution was quickly filtered through a Pyrex brand coarse fritted glass filter. The solid was discarded. The liquid phase was separated into two portions of approximately equal volumes each of which was placed in 1000 ml erlenmeyer flask containing a stirring bar and a marble. Each portion of the liquid phase ranged from 250 to 450 ml.

ii. Preparation of near-duplicate complexes

To one portion of the saturated liquid solution prepared as described in (a. i.) above, a known amount of KI was added which had been rapidly crystallized from water to obtain a small particle size. To the other flask was added a known amount of KBr prepared in a similar manner. The amount of solid added in both cases ranged from one to three grams.

The flasks were now stoppered, sealed in rubber, placed in the constant temperature bath with stirrers turned on, and the flasks shielded from the light, all as described previously.

After periods of time ranging from approximately two to three weeks the stirring was stopped. A 5 ml portion of the liquid phase from each of the flasks was pipetted off for analysis.

The mixtures were quickly suction filtered through a coarse Pyrex brand fritted glass filter. The solutions in the flasks were swirled while filtering to facilitate the collection of as much of the solid phases as possible.

The solid phases were then analyzed.

b. Near duplicate complexes by the method of the infinitesimal approach to the limiting miscibility

i. Procedure

The procedure is similar to the method of near-duplicate complexes of arbitrary composition described above in section (1. a.), the only difference is that here the saturated liquid solution that is initially prepared is the KI-KBr-H₂O isothermally invariant solution at 25°C.

ii. Method of preparation of the isothermally invariant liquid solution when the composition is unknown

A saturated KI-KBr-H₂O liquid solution was prepared at 25°C at an

arbitrary mole ratio of the dissolved salts. The supersaturated solution was placed in the constant temperature bath and the solid phase that crystallized out collected. The time allowed before a sample of the solid phase was taken varied from several minutes to several hours. No attempt was made at this point to completely relieve the supersaturation.

The crystals were dried either by being placed in an oven at 100°C or by being placed in a vacuum dessicator for lengths of time varying from several hours to overnight.

A sample of the crystals was then dropped into a test tube containing 1,1,2,2-tetrabromoethane supplied by Eastman Organic Chemicals. The test tube was left undisturbed until the crystals had come to rest. This time varied from several minutes to several hours. If the crystals had come to rest near the top of the test tube the mole ratio of the solution was then shifted by addition of more KI and water and the solution was again supersaturated and the procedure repeated. If the crystals had come to rest near the bottom of the test tube more KBr and water were then added to the original solution and the procedure was again repeated.

By reducing the quantity of salt added to the solution before each float and sink trial, the addition of only several grams of the appropriate salt caused the float and sink test to yield either floating or sinking crystals. Upon further decreasing the amount of salt added before each float and sink test, a situation was soon reached where the crystals obtained were of the two types that both float and sink.

This mixture was then placed in the constant temperature bath with stirring to obtain a saturated solution. The time varied from two to seven days. At this point a 5 ml sample of the liquid phase was removed for analysis. This analysis yielded the composition of the isothermally

composition-invariant liquid solution.

iii. Method of preparation of the isothermally invariant liquid solution when the composition is known

Utilizing the results of the analysis of the liquid phase described in section (ii) above, KI, KBr, and H₂O were added to an erlenmeyer flask in known appropriate amounts to prepare a ternary phase system. The prepared mixture was first supersaturated at 25°C and left stirring several days. At that time, a sample of the solid phase was tested using the float and sink method to make sure both floating and sinking particles were present. The liquid solution was quickly filtered. This was an isothermally composition-invariant liquid solution.

2. Metastable equilibrium by the method of isothermal relief of supersaturation in the system KI-KBr-H₂O at 25°C

An isothermally invariant solution is prepared at 25°C as described in the last section (1. b. iii). Added to this solution of a volume which ranged from approximately 180 ml. to 500 ml. in a 1000 ml. flask is a carefully weighed amount of from .5 grams to 5 grams of either KI or KBr. The mixture was then placed on a hotplate and gently warmed with constant agitation for several minutes until all of the solid had gone into solution. The erlenmeyer flask was then placed in a constant temperature bath and allowed to cool down undisturbed to 25°C while the temperature was observed by having a thermometer in the flask. The thermometer used was encased in smooth glass to avoid sites for possible nucleation of solid phases.

Care was taken to ensure that no crystals had appeared before the solution temperature had actually reached 25°C. In the cases where nucleation was observed to take place at a temperature higher than 25°C, the mixture was removed from the constant temperature bath and all of the crystals redissolved

by gently warming on a hotplate. The crystallization procedure was then repeated from this point. The water bath used was large enough so that the addition of the warm beaker into it caused no observable effect on the temperature of the bath.

Depending upon both the degree of supersaturation of the solution and the amount of agitation and/or stirring of the complex, crystals could be seen to first appear after periods of time ranging from several minutes to having not appeared at all after 24 hours. In the latter case, relief of supersaturation was induced either by seeding the solution or by agitation of the flask. Various combinations of amount of agitation of the flask, degree of supersaturation, and composition of the solid solution seed crystals of KI-KBr were used.

In one experiment, an isothermally invariant solution was supersaturated and then divided into two portions. In one portion the supersaturation was relieved with constant stirring and the other part the flask remained undisturbed.

After varying lengths of time ranging from eight hours to one week depending upon the conditions of each individual experiment, a 5 ml. sample of the liquid phase was pipetted off for analysis. The complex was then filtered as described earlier and the solid phase was analyzed.

3. KI-KBr at 94°C by the method of isothermal evaporation

Various mole ratios of KI and KBr salts were weighed to the nearest mg. into a 250 ml. beaker that was in the constant temperature bath at 100°C. The weight of the combined salts was approximately 100 grams.

To the 250 ml. beaker was added a sufficient amount of boiling distilled water to completely dissolve all of the solid. The beaker was covered. This arrangement remained for a time period from one half hour to eight hours with occasional stirring with the thermometer. The temperature of both beakers

was observed occassionally. The temperature of the outer beaker was always 100°C. The temperature of the 250 ml. beaker rose to approximately $94.0 \pm 1.^\circ\text{C}$ uniformly throughout the beaker and remained constant.

When an amount of solid had appeared that is estimated to be between .5 and 2 grams, a spatula was inserted into the beaker and sample of the solid phase quickly removed. This step had to be accomplished quickly because a layer of new solid would start to form on the top surface of the solution immediately upon removing the cover glass to insert the spatula.

The solid was immediately dried in several layers of filter paper that had been warmed previously in an oven at 94°C. After five to ten minutes the solid was placed into a powder pattern camera and an x-ray powder photograph was taken.

Several variations of the procedure described here were also investigated. In exploratory investigations, crystals were removed several times from the same solution as each fraction crystallized out. Also, the solution was at times filtered through a steam jacketed filter to obtain the crystals, crystals were dried in an oven at 94°C on filter paper, and crystals were dried on both hot porous and non-porous plates in an oven at temperatures ranging from 94°C to 110°C.

4. NH₄I -KI-third component at 25°C by the method of duplicate complexes

1.24 grams NH₂·H₂SO₄ and .6 grams NaOH were dissolved in 1000 ml. of distilled water and the solution thoroughly mixed. This was the third component used for the study of this system. The NH₂·H₂SO₄ was supplied by the J. T. Baker Co. The NaOH was supplied by Matheson Coleman and Bell.

Two complexes of identical gross composition (or, in some cases, within two mole per cent of each other in gross composition of added salts) were prepared in various mole ratios. KI weighed to the nearest mg. was added to a 1000 ml. erlenmeyer flask. Added to this solid was a pipetted sample of

the third component solution that had been prepared that same day. The volume of the third component ranged from 150 ml. to 240 ml.

A marble and a teflon brand coated magnetic stirring bar were placed in the flask. The solid was dissolved by stirring the flask on a magnetic stirrer for five to ten minutes. The flask was then placed in a constant temperature bath at 25°C and allowed to come to thermal equilibrium with the bath. After ten to fifteen minutes, NH_4I weighed to the nearest mg. was added to the flask. The amount of solid added to the flask was such, that at equilibrium, approximately 20 to 50 grams of the salts remained in the solid phase.

A similar procedure was repeated with identical amounts or nearly identical amounts of the three components with the order of addition of the salts reversed. When KI was added last, it was first recrystallized rapidly from water to obtain small crystal sizes.

The flasks were stoppered with ground glass caps surrounded with rubber and stirring with marbles started, as described earlier. Stirring was continued for periods ranging from 12 to 21 days. At the end of this time, the solid phase was analyzed.

The solubility of pure NH_4I in the solvent used in this study was determined by approaching equilibrium from two directions. The solvent and NH_4I were added together in known amounts in duplicate.

One beaker was placed in the temperature bath and allowed to warm up to 25°C. The beaker was left stirring for 5 days. This is an approach to equilibrium from undersaturation.

The other beaker was gently warmed to 30°C for about 30 minutes with swirling. This beaker was then left with stirring for three days. This is an approach to equilibrium from oversaturation.

II C. Chemical Analysis

1. System KI-KBr-H₂O at 25°C

a. Analysis of liquid phase

i. Weight per cent salt in liquid phase

The liquid phase of the KI-KBr-H₂O complex at 25°C was analyzed gravimetrically for weight per cent salt by evaporation of H₂O.

The complex that was analyzed was left unstirred for at least one hour before a sample of the liquid phase was removed for analysis. Five ml. of the solution to be analyzed was pipetted into a tared erlenmeyer Exax brand 100 ml. weighing bottle with a ground glass cap that fit on the outside of the bottle. Care was taken to keep the pipette away from near the bottom of the erlenmeyer flask which contained the complex in order to avoid suctioning any fine crystals into the pipette along with the liquid phase. The cap was quickly placed on the weighing bottle and the weight of the bottle determined.

The sample was then dried in an oven at 60 to 80°C for approximately four or five hours until no liquid could be seen. The oven temperature was then raised to between 120 and 140°C and the sample dried to constant weight.

From the weight of the liquid solution and the weight of the dried salt in the solution, the weight per cent salt was determined. The solid that remained was ground with a metal spatula and redried at 120 to 140°C for one to two hours for subsequent use in analyzing for the Br⁻ - I⁻ ratio. in solution.

Saturated solutions of the pure components KI and KBr prepared by the method of isothermal relief of supersaturation were each analyzed in duplicate for weight per cent salt and the values obtained were compared with literature values.

ii. Analysis for Br⁻ in presence of I⁻ in liquid phase

The method of analysis is a modification of one suggested by Erdey.⁴ Each unknown was analyzed in either duplicate or triplicate. For each group of unknowns that were analyzed a known sample of similar gross composition prepared from the pure components was also analyzed at the same time. This acted as a constant check on the analytical procedure and was used to calibrate the results of the analysis. The supplier and quality of each of the chemicals used in this analysis is given in table II 1.

Samples of the dried salt were carefully weighed into 1000 ml. wide-mouth beakers. The average sample size was approximately .5 grams and the range was .3 to 1 gram. The samples were diluted to 700 ml. with distilled water. Added to the beakers with stirring was 25 ml. of 10% NaNO₃. Added slowly was 3 ml. 1:1 H₂SO₄. The resulting orange-red solutions were placed on hotplates and boiled uncovered. The boiling was continued until thirty minutes after the color had disappeared. The beakers were then allowed to cool. The solutions were tested for the complete removal of I⁻ by the addition of several ml. of 10% NaNO₃ and a few drops of 1:1 H₂SO₄. Slowly added to the cool solution was 5% AgNO₃ in the amount needed to coagulate the precipitate. Then a few drops more 5% AgNO₃ were added. The solution was heated until clear. To the cooled solution was added a few drops 5% AgNO₃ to test for complete precipitation.

The precipitate was washed several times with dilute nitric acid (one to three ml. per liter water). The precipitate was transferred into a tared porous porcelain crucible and washed with dilute nitric acid solution until free of Ag⁺ ion. The washings were tested with a few drops HCl until no cloudiness appeared. The precipitate was then washed with 1% acetic acid, and dried at 110 to 120°C to constant weight.

TABLE II 1.

Chemicals used in analysis for Br⁻ in the presence of I⁻

<u>Chemical</u>	<u>Supplier</u>	<u>Quality +</u>
Glacial Acetic Acid	E. I. Dupont De Nemours and Co., Inc.	
Hydrochloric Acid	E. I. Dupont De Nemours and Co., Inc.	
Nitric Acid	J. T. Baker Chemical Co.	Baker Analyzed Reagent
Silver Nitrate	Mallinckrodt Chemical Works	Analyzed Reagent
Sodium Nitrite	Merck and Co.	
Sulfuric Acid	E. I. Dupont De Nemours and Co., Inc.	

+ All chemicals met A. C. S. specifications

From the weight of the dried salts and the weight of the AgBr precipitate, the KI-KBr ratio was calculated for each sample.

b. Analysis of solid phase and wet residue

i. Weight per cent salt in solid phase and wet residue

The complexes were filtered through a coarse Pyrex brand fritted glass filter under suction. The moist solid was left on the suction filter to drain one to two minutes. As much of the solid phase (or phases) as possible was transferred with the aid of a spatula to #595 filter paper supplied by Schleicher and Schuell Co. The solid was wrapped inside three or four sheets of filter paper. After approximately two minutes, the moist solid was transferred to fresh filter paper. The bulk of the moist solid was quickly placed into two or three weighing bottles five ml. in volume with caps that had ground glass seals. Sample size ranged from .3 to 1 gram. The remainder of the solid was left on the filter paper and placed into a vacuum dessicator for approximately twelve hours to dry for subsequent x-ray analysis.

The weighing bottles were quickly weighed and then dried at 110 to 120°C to constant weight. From the weight of each moist and dry sample and from the results of the analysis of the conjugate liquid phase, the amount of salt left behind by evaporation of the H₂O in the wet residue was determined.

ii. Analysis of Br⁻ in the presence of I⁻ in solid phase and wet residue

The solid samples remaining in section (i) above were analyzed to determine the Br⁻ - I⁻ ratio as outlined in section (a. ii). The samples were transferred quantitatively from the weighing bottles to the 1000 ml. beakers. A layer of solid was often seen to deposit on the bottom and wall

of the weighing bottle during the drying process. Care was taken to wash the weighing bottle several times with distilled water and then to add this distilled water to the 1000 ml. beaker to ensure that all of the sample was transferred.

2. System KI-NH₄I-third component at 25°C

The complexes were quickly filtered through a Pyrex brand fritted glass filter and left to drain approximately two minutes. As much of the solid phase as possible was transferred to #595 filter paper supplied by Schleicher and Schuell Co. and wrapped inside three or four sheets. After approximately two minutes, the moist solid was transferred to fresh filter paper. Three samples of the moist solid phase ranging from 1.8 to 4 grams were placed in tared covered Coors brand crucibles and weighed. The solid that remained was placed into a tared weighing bottle and weighed.

The samples were dried at 80 to 90°C for five hours and were then weighed. They were then dried for an additional hour and reweighed.

The dried crucibles were placed into a furnace at approximately 500°C and heated to constant weight. From the information obtained and from the known gross composition of the complex, the compositions of the liquid and solid phases were determined.

A sample of KI-NH₄I solid solution prepared and analyzed previously by two independent methods in this laboratory was analyzed as a check of the analytical procedure.⁵

D. X-ray analysis

1. Powder equipment and sample handling

The powder patterns were prepared with an x-ray diffraction unit of type 12045/3 and serial no. D4-376-7 manufactured by Philips Electronic Instruments. The camera employed was a Philips Debye-Scherrer powder

camera no. 52056-B and serial no. 50-35 of 114.59 mm. diameter. Nickel filtered CuK radiation was used. The film was mounted in the camera in the Ievins-Straumanis asymmetric method.⁶ The film was Kodak No-Screen Medical X-ray film no. NS-392T and was cut to uniform size with a Philips Film Punch and Cutter. Exposure time varied depending on the sample but was usually 12 hours. Film handling and dark room procedures followed that described by Shoemaker and Garland.⁷ After films were developed and air dried, they were read with a Norelco brand comparator.

The x-ray unit employed is equipped with three cameras and three camera tracts. Only one camera and one tract were used to prepare all powder patterns in order to facilitate reproducibility.

Dried samples were ground with an agate mortar and pestle. A sample of the solid was placed into an x-ray capillary tube of .5 mm. diameter and 1/100 mm wall thickness. Capillaries were supplied by the Unimex-Caine Corp. All photographs were taken at room temperature, which averaged near 27°C.

2. X-ray analysis of the System KI-KBr at 94°C and of NH₄I-KI system at 25°C

Solid solutions of KI-KBr prepared at 94°C were analyzed for composition by x-ray techniques. To calibrate the x-ray methods, powder photographs of KI-KBr solid solutions prepared at 25°C were also taken. By comparison of the results of the chemical analysis with the results of the x-ray analysis, a calibration was obtained for use in determining the composition of the solid solutions prepared at 94°C.

Quality of all patterns was noted as an indication of homogeneity and crystal size of samples. Several samples of KI-NH₄I solid solutions were also analyzed by x-ray methods.

Powder photographs were taken of the pure components KI, KBr, and NH_4I . For KI and KBr, the samples were first crystallized from water to obtain small particle size.

CHAPTER III. DATA ANALYSIS AND RESULTS

A. KI-KBr-H₂O at 25°C

1. Analytical method

a. Gravimetric analysis

The KI-KBr mole ratios were determined by the oxidation of I⁻ to I₂ by nitrous acid and the subsequent precipitation of Br⁻ as AgBr. The mole ratios of I⁻ and Br⁻ that were of concern in this study were those corresponding to two different ranges of composition. Compositions similar to that of the limits of the solid-solid solubility on both sides of the miscibility gap at 25°C were of interest. Also of interest were the mole ratios in the vicinity of the composition of the dissolved salts in the isothermally invariant liquid solution. This mole ratio, however, is similar to that of the limiting solid-solid solubility of β-phase crystals.

Samples prepared in known weight ratios of KI and KBr were analyzed in the ranges of interest. The data obtained from the analysis of the known samples enabled an improving factor to be determined that increased the accuracy of the analytical procedures. This empirical relationship that was determined was found to hold for both of the composition ranges being studied.

The details of the analysis of samples of known composition are summarized in Table III 1.

Columns 2 and 3 list the weight in mgs. of the KI and KBr that was analyzed. Column 4 lists the experimentally obtained weight of the AgBr precipitates. It was found that the KBr weight determined experimentally was almost always higher than the weight of the KBr actually present (the one exception is sample no. 28). The weight of the KBr calculated from the weight of the AgBr precipitate minus the weight of the KBr actually present is shown in mgs. in column 5.

Column 5 is the basis for an improving factor for the analytical procedure. The average value in column 5 is 1.5 mgs. KBr. The weight of 1.5 mgs. KBr corresponds to 2.4 mgs. of AgBr precipitate. Thus, to obtain a more accurate analysis, 2.4 mgs. was subtracted from each AgBr weight experimentally obtained. The weight per cent KBr present in each sample is shown in column 6. The weight per cent KBr found experimentally by first subtracting the 2.4 mg. improving factor from the weight of the AgBr precipitate is shown in column 7.

Column 8 lists the difference between the weight per cent KBr obtained by the analysis with the improving applied minus the actual weight per cent KBr of the sample.

Sample nos. 1 to 31 correspond to weight ratios in the range 9.28% KBr to 36.86% KBr. This is the range of the composition of the limiting β -phase solid solution and the ratio of dissolved salts near the isothermally invariant liquid solution. Sample nos. 32 to 38 correspond to weight ratios in the range of composition 75.25% KBr to 95.19% KBr. This is the range of composition of the limiting α -phase solid solution.

It is worthy of note that the improving factor of 1.5 mgs. KBr determined for the analysis is found to be the same whether the average value of column 5 is determined using all of the samples or whether samples nos. 1 to 31 and 32 to 38 are calculated separately. The fortuitous agreement emphasizes that the improving factor is constant throughout the entire range of composition.

The average deviation determined by averaging the values in column 8 is found to be $\pm .09$ weight %.

In determining the composition of the KI-KBr complexes, the improving factor has been applied to all the data.

TABLE III (1)

Analysis of Known Samples of Mixtures of KI and KBr

1	2	3	4	5	6	7	8
Sample	KI	KBr	AgBr	KBr Calculated	Weight	Weight	Col. 7
No.	(mg)	(mg)	(mg)	from Col. 4 minus	% KBr	% KBr by	minus
				Weight in Col. 3		Analysis	Col. 6
1	903.8	92.5	146.4	0.3	9.28	9.16	-.12
2	886.5	109.4	178.0	3.4	10.99	11.18	+.19
3	412.0	62.4	101.3	1.8	13.15	13.22	+.07
4	866.7	133.1	212.2	1.4	13.31	13.30	-.01
5	588.5	87.7	144.4	3.8	12.97	13.31	+.34
6	508.9	79.6	128.1	1.6	13.53	13.54	+.01
7	508.5	89.5	143.2	1.3	14.97	14.92	-.05
8	634.7	121.7	194.3	1.4	16.09	16.08	-.01
9	1293.6	273.1	433.5	1.7	17.43	17.44	+.01
10	687.1	163.2	260.1	1.7	19.19	19.20	+.01
11	778.8	186.7	297.3	1.7	19.34	19.36	+.02
12	664.8	160.3	256.9	2.5	19.43	19.55	+.12
13	670.5	164.7	261.4	1.0	19.72	19.66	-.06
14	592.1	144.7	232.6	2.7	19.64	19.80	+.16

continued on next page.....

TABLE III (1) (cont.)

Analysis of Known Samples of Mixtures of KI and KBr

1	2	3	4	5	6	7	8
Sample	KI	KBr	AgBr	KBr Calculated from Col. 4 minus Weight in Col. 3	Weight % KBr	Weight % KBr by Analysis	Col. 7 minus Col. 6
No.	(mg)	(mg)	(mg)				
15	491.1	120.9	194.0	2.1	19.75	19.84	+.09
16	383.4	99.0	158.4	1.4	20.52	20.50	-.02
17	626.7	171.3	270.4	0.1	21.47	21.29	-.18
18	609.6	173.5	277.1	2.1	22.16	22.23	+.07
19	456.7	134.7	213.8	0.8	22.78	22.66	-.12
20	636.9	190.0	301.4	1.0	22.98	22.92	-.06
21	897.8	272.4	433.8	2.5	23.28	22.36	+.08
22	550.0	169.7	270.7	1.9	23.58	23.62	+.04
23	368.8	121.8	195.2	1.9	24.84	24.92	+.08
24	613.0	205.1	324.7	0.7	25.07	24.97	-.10
25	573.1	198.4	314.8	1.1	25.72	25.66	-.06
26	473.0	172.9	274.0	0.8	26.77	26.64	-.13
27	633.2	236.9	375.9	1.3	27.23	27.20	-.03

continued on next page.....

TABLE III (1) (cont.)

Analysis of Known Samples of Mixtures of KI and KBr

1	2	3	4	5	6	7	8
Sample No.	KI (mg)	KBr (mg)	AgBr (mg)	KBr Calculated from Col. 4 minus Weight in Col. 3	Weight % KBr	Weight % KBr by Analysis	Col. 7 minus Col. 6
28	780.1	297.0	467.2	- .9	27.57	27.35	- .22
29	367.5	157.1	249.7	1.2	29.95	29.87	- .08
30	372.0	167.7	266.9	1.5	31.07	31.05	- .02
31	558.5	326.0	516.8	1.5	36.86	36.86	.00

32	156.4	475.5	751.8	1.0	75.25	75.17	- .08
33	85.9	552.7	872.7	0.4	86.55	86.38	- .17
34	103.7	829.3	1311.5	1.9	88.89	88.93	+ .04
35	62.8	590.5	934.4	1.7	90.39	90.42	+ .03
36	44.3	450.4	711.2	0.4	91.05	90.80	- .25
37	49.2	497.0	759.5	2.4	90.69	90.84	+ .15
38	30.4	601.1	953.0	2.9	95.19	95.41	+ .22
				1.5 average for column 5			+ 0.09 average for column 8

b. Weight per cent salt

Saturated solutions of KI and of KBr were prepared by the method of isothermal relief of supersaturation. The liquid solutions in both cases were left with stirring in the presence of a solid phase for at least 3 days. The weight per cent salt was determined twice for each solution with at least one day with no additional stirring between the two determinations.

Shown in table III 2 are the values obtained in the present study for the weight per cent salt in saturated solution for the pure components. Also shown are values felt to be reliable that have been obtained by workers employing an isopiestic method.

By reference to table III 2, the precision obtained for analysis of weight per cent salt is seen to be greater than one part per thousand. The agreement with other workers is within .3 per cent.

2. Results of Analyses

The data obtained for the system KI-KBr-H₂O at 25°C are shown in table III 3. Columns 2 and 3 list the weight per cent of each of the dissolved salts contained in the saturated liquid phase. The average deviation for each of the analyses is shown. Column 4 lists the weight in grams of the dissolved salts per 100 grams solution.

Columns 5, 6, and 7 show the compositions in weight per cent for each of the components obtained from the individual analyses of the moist solid samples.

The amount of dissolved salts carried with the weight per cent H₂O listed in column 7 was calculated using the data in columns 2, 3, and 4. The method of the wet residue was then applied to the data in columns 5, 6, and 7 to calculate the composition of the solid phase alone. This is shown in columns 8 and 9. The average deviation of the analysis for

TABLE III 2

Weight per cent salt and molality in saturated water
solution at 25°C for Pure Components

	Present Work		Other Workers	Ref.
	Weight % salt	m	m	
KBr	40.59	5.741	5.736	8
	40.60	5.743		

KI	59.79	8.957	8.98	9
	59.79	8.957		

the composition of the solid phase is shown.

Column 10 lists the method of preparation of each complex. The methods of preparation are abbreviated on the chart as follows:

IRS	isothermal relief of supersaturation
NDC	near duplicate complexes
IALM	infinitesimal approach to the limiting miscibility

The direction from which equilibrium was approached for complexes prepared by the method of near duplicate complexes is also shown in Column 10. For example, NDC-KBr represents a complex in which pure KBr was added to a saturated solution and left to reach equilibrium. Similarly, NDC-KI represents a complex in which pure KI was added to a saturated solution.

IALM-NDC represents a sample in which the saturated solution before any solid was added to the complex was of the isothermally invariant liquid composition.

Column 10 also indicates for samples prepared by the method of isothermal relief of supersaturation which salt was added to the isothermally invariant solution. For example, IRS-KI indicates pure KI was added to the isothermally invariant solution. IRS-KBr indicates that the pure KBr was added to the isothermally invariant solution.

Column 11 lists the type of solid phase(s) present in each complex.

Complexes labelled Q and S were prepared by the addition of both pure KI and KBr to a saturated solution. It is not possible in this range of mole fraction of dissolved salts to prepare complexes by the addition of only pure KI to a saturated solution. This can be seen from table III 3 column 4 in which the solubility of the combined salts is

TABLE III (3)

Experimental Results for KI-KBr-H₂O at 25°C

1	2	3	4	5	6	7	8	9	10	11		
Weight % Dissolved Salts			Grams Salt per 100 grams Solution	Weight % Solid Phase and Wet Residue			Weight % Solid Phase Alone			Method	Crystal	
<u>KI</u>	<u>KBr</u>	<u>+</u>		<u>KI</u>	<u>KBr</u>	<u>H₂O</u>	<u>KI</u>	<u>KBr</u>	<u>+</u>			
A	100.00	0.00	---	59.79	---	---	---	100.00	00.00		IRS	pure KI
B	85.16	14.84	.12	59.81	90.09	8.48	1.43	91.54	8.46	.01	NDC-KI	β-phase
					89.93	8.47	1.60				B-C	
C	84.87	15.08	.03	59.82	90.46	9.11	.43	91.08	8.92	.12	NDC-KBr	β-phase
					90.46	8.80	.74				B-C	
					90.39	8.86	.75					
D	82.27	17.73	.08	59.79	86.37	12.11	1.52	87.75	12.25	.09	NDC-KI	β-phase
					86.38	12.13	1.49				D-E	
					86.22	12.32	1.46					
E	82.00	18.00	.07	59.77	85.59	12.84	1.57	87.08	12.92	.04	NDC-KBr	β-phase
					85.47	12.89	1.64				D-E	
					85.64	12.77	1.59					
F	81.60	18.40	.01	59.77	85.93	12.96	1.11	86.79	13.21	.17	IALM-NDC-KI	β-phase
					85.89	13.43	.68					
					86.42	13.12	.46					

continued on next page.....

TABLE III (3) (continued)

Experimental Results for KI-KBr-H₂O at 25°C

1	2			3	4	5			6			7	8			9	10	11
	Weight % Dissolved Salts					Grams Salt per 100 grams Solution	Weight % Solid Phase and Wet Residue			Weight % Solid Phase Alone			Method	Crystal				
	<u>KI</u>	<u>KBr</u>	<u>+</u>		<u>KI</u>	<u>KBr</u>	<u>H₂O</u>	<u>KI</u>	<u>KBr</u>	<u>+</u>		<u>KI</u>	<u>KBr</u>	<u>+</u>				
G*	81.52	18.48	.19	59.76	86.20	13.35	.45	86.52	13.48	.11	IRS-KI	non-equilibrium β-phase						
					86.10	13.58	.32											
H	81.60	18.40	.15	59.78	84.33	13.74	1.93	86.10	13.90	.02	NDC-KI H-P	α + β-phases						
					84.13	13.76	2.11											
I*	81.79	18.21	.14	59.76	84.78	14.96	.26	85.00	15.00	.01	IRS-KI	non-equilibrium β-phase						
					84.83	14.99	.18											
J	81.44	18.56	.04	59.78	84.20	14.85	.95	85.04	14.96	.02	IRS-KBr	metastable β-phase						
					84.01	14.86	1.13											
K	81.25	18.75	.07	59.79	84.39	15.29	.32	84.68	15.32	.00	IRS-KBr	metastable β-phase						
					84.34	15.28	.38											
L	81.66	18.34	.03	59.79	84.83	15.17	.07	84.84	15.16	.01	IRS-KI	non-equilibrium β-phase						
					84.85	15.15	.07											
M	80.69	19.31	.17	59.77	82.81	16.94	.25	83.02	16.98	.01	IRS-KBr	metastable β-phase						
					82.72	16.95	.33											

*Complexes G and I were prepared from the same supersaturated solution

continued on next page.....

TABLE III (3) (continued)

Experimental Results for KI-KBr-H₂O at 25°C

1	2	3	4									10	11			
			Weight % Solid													
			Weight %			Grams Salt per 100 grams Solution	Phase and Wet Residue			Weight % Solid Phase Alone				Method	Crystal	
			Dissolved Salts				KI	KBr	H ₂ O	KI	KBr					±
<u>KI</u>	<u>KBr</u>	<u>±</u>		<u>KI</u>	<u>KBr</u>	<u>H₂O</u>	<u>KI</u>	<u>KBr</u>	<u>±</u>							
N	81.44	18.56	.01	59.76	52.51 52.60	44.43 44.26	3.06 3.14	52.88	47.12	.05	IRS-KBr	α + β-phases				
O	81.45	18.55	.02	59.76	18.52 18.58 18.57	79.15 79.34 79.80	2.33 2.08 1.63	16.97	83.03	.23	IALM-NDC-KBr	α-phase				
P	81.31	18.69	.15	59.67	17.93 17.85 17.66	79.21 79.24 79.52	2.86 2.91 2.82	15.44	84.56	.08	NDC-KBr H-P	α-phase				
Q	80.27	19.73	.09	59.26	19.61 19.20	74.60 74.41	5.79 6.39	14.45	86.55	.47	NDC-KI-KBr Q-R	α-phase				
R	80.11	19.89	.10	59.20	18.33 18.80 18.49	76.37 76.28 76.62	5.30 4.92 4.89	14.47	85.53	.32	NDC-KBr Q-R	α-phase				
S	78.86	21.14	.02	58.57	15.43 15.23 15.04	81.74 81.49 81.55	2.83 3.28 3.41	12.67	87.33	.34	NDC-KI-KBr S-T	α-phase				
T	78.47	21.53	.11	58.50	14.70 14.60	82.12 82.24	3.18 3.16	12.07	87.93	.04	NDC-KBr S-T	α-phase				
U	00.00	100.00		40.60	----	----	----	0.0	100.00		IRS	pure KBr				

seen to increase at higher KI mole ratios. The addition of several grams pure KI to a saturated solution would result, at equilibrium, in little or no salt remaining in the solid phase.

Table III 4, 5, and 6 list the mole % dissolved salts in the liquid phase and the mole % of each component in the solid phase.

The saturated solutions that were prepared initially to have KI and KBr added to them for the method of near duplicate complexes were analyzed for the KI-KBr mole ratio and for weight per cent salt. The weight of the KI or KBr added and the weight of the equilibrium solid obtained were recorded. A mass balance calculation was then performed to insure that the chemical analyses were in agreement with the mass balance. In all cases, the agreement was within the combined limits of the errors of the chemical analyses. A sample of such a calculation is shown in table III 7.

Various combinations of experimental variables were employed to prepare the complexes by the method of isothermal relief of supersaturation.

Complexes G and I were prepared in the following manner:

3.4 grams KI were added to approximately 450 ml of the isothermally invariant liquid solution. The solution was warmed to dissolve the solid as described in the experimental section. At this point, the solution was separated into two beakers each containing approximately equal volumes of the warm solution. Both portions were placed into the constant temperature bath and allowed to reach 25°C.

One portion, labelled I, was placed into the constant temperature bath with no stirring and left overnight. The next morning no crystals were observed. The beaker was shaken for several minutes and then left 10 days unstirred before the complex was analyzed.

TABLE III (4)

KI-KBr-H₂O at 25°CMole Per Cent Dissolved Salts and Solid PhaseEquilibrium Data

	<u>Mole Per Cent Dissolved Salts in Liquid Phase</u>			<u>Mole Per Cent Salts in Solid Phase</u>			Crystal
	KI	KBr	±	KI	KBr	±	
A	100.00	0		100.00	0.0		pure KI
B	80.45	19.55	.15	88.58	11.42	.01	β-phase
C	80.14	19.86	.04	87.97	12.03	.16	β-phase
D	76.89	23.11	.10	83.71	16.29	.10	β-phase
E	76.56	23.44	.09	82.85	17.15	.05	β-phase
F	76.06	23.94	.01	82.48	17.52	.17	β-phase
H	76.07	23.93	.18	81.62	18.38	.03	α + β-phases
N	75.88	24.12	.01	44.58	55.42	.05	α + β-phases
O	75.89	24.11	.02	12.78	87.22	.18	α-phase
P	75.72	24.28	.24	11.58	88.42	.07	α-phase
Q	74.46	25.54	.11	10.80	89.20	.41	α-phase
R	74.28	25.72	.12	10.82	89.18	.25	α-phase
S	72.78	27.22	.03	9.42	90.58	.26	α-phase
T	72.32	27.68	.13	8.96	91.04	.03	α-phase
U	0.00	100.00		00.00	100.00		pure KI

TABLE III (5)

KI-KBr-H₂O at 25°C

Mole Per Cent Dissolved Salts and Solid Phase

Metastable Equilibrium

	<u>Mole Per Cent Dissolved Salts in Liquid Phase</u>			<u>Mole Per Cent Salts in Solid Phase</u>		
	KI	KBr	<u>±</u>	KI	KBr	<u>±</u>
J	75.87	24.13	.04	80.30	19.70	.02
K	75.66	24.34	.08	79.85	20.15	.00
M	74.98	25.02	.20	77.80	22.20	.02

TABLE III (6)

KI-KBr-H₂O at 25°C

Mole Per Cent Dissolved Salts and Solid Phase

Non-Equilibrium

	<u>Mole Per Cent Dissolved Salts in Liquid Phase</u>			<u>Mole Per Cent Salts in Solid Phase</u>		
	KI	KBr	<u>±</u>	KI	KBr	<u>±</u>
G	75.97	24.03	.24	82.14	17.86	.14
I	76.30	23.70	.17	80.24	19.76	.02
L	76.14	23.86	.03	80.05	19.95	.01

TABLE III (7)

Sample Calculation: Mass balance for complexes D and E

A saturated solution of approximately 800 ml. was analyzed. The solution was divided into two parts of approximately equal volumes labelled D and E. To beaker D was added 2.0 grams KI and to beaker E was added 1.7 grams KBr. After one month with at least two weeks stirring with marbles, both complexes were analyzed. Approximately 2 grams solid was collected from each beaker at equilibrium.

By taking into account the composition of the initial liquid phase, the number of grams of the salt that was added to each beaker, and the weight of the solid phase obtained at equilibrium and the analysis of that solid, the composition of the final liquid solution was calculated. Comparison of the calculated values with the experimental values show excellent agreement.

<u>Experimental</u>	<u>H₂O</u>	<u>weight %</u>		<u>disolved salts</u>	
		<u>KI</u>	<u>KBr</u>	<u>KI</u>	<u>KBr</u>
<u>Liquid solutions</u>					
Solution initially	40.22	49.21	10.59	82.32	17.68 ⁺ .08
<u>Solution at equilibrium</u>					
D	40.21	49.19	10.60	82.27	17.73 ⁺ .08
E	40.23	49.01	10.76	82.00	18.00 ⁺ .07
<u>Solid Solution</u>					
D				87.75	12.25 ⁺ .09
E				87.08	12.92 ⁺ .04
<u>Calculated</u>					
<u>Solution at equilibrium</u>					
D	40.22	49.24	10.54		
E	40.24	48.97	10.80		

The other portion, labelled G, was left stirring to relieve the supersaturation for two days. The complex was then analyzed.

By reference to tables III 3 and 6, it can be seen that the compositions of the solid phases obtained in the two cases are different even though the supersaturated liquid phases were identical.

Complex J was prepared by seeding a supersaturated solution with seed crystals of composition 10 mole% KI. The complex was left stirring for three days and then analyzed.

The details of the preparation of complex K are discussed as being representative of the method of isothermal relief of supersaturation. The supersaturated solution as well as the final saturated solution were analyzed.

An isothermally invariant liquid solution was prepared of approximately 450 ml. To this solution was added 1.1 grams KBr and the solution was supersaturated. The solution was kept stirring for two days at 25°C. The results of the analyses are shown below.

	mole %		grams salt per
	KI	KBr	100 grams solution
isothermally invariant solution:	75.92	24.08 ± .03	59.77
supersaturated solution:	75.65	24.35 ± .21	59.83
saturated solution:	75.66	24.34 ± .08	59.79
solid phase:	79.85	20.15 ± .00	-----

Complex L was prepared by relieving the supersaturation with only occasional stirring for two days.

Complex M was prepared with no stirring. The complex was analyzed

after one night.

The details of the preparation of complex N will be discussed in detail. This is because the solid obtained was of two phases and also because an analysis was performed on the supersaturated solution as well as the final saturated solution.

An isothermally invariant solution was prepared of approximately 500 ml. To this solution was added 1.2 grams KBr. The solution was then supersaturated at 25°C. The supersaturated solution was seeded with α -phase seed crystals and left stirring for one week. The results of the analysis are shown.

	mole %		grams salt per
	KI	KBr	100 grams solution
isothermally invariant solution:	76.06	23.94 \pm .02	59.77
supersaturated solution:	75.80	24.20 \pm .15	59.85
Saturated solution:	75.88	24.11 \pm .01	59.76
solid phase:	44.58	55.42 \pm .05	-----

* * *

The analysis of α -phase crystals shows a larger deviation than that obtained for the β -phase crystals. This is attributed primarily to the influence of the wet residue on the analysis of the composition of the solid phase.

The application of the method of the wet residue for the β -phase had only a minor effect on the composition as compared to the effect of the method on the analysis for the α -phase crystals. There are two reasons for this difference.

The first difference arises from the differing natural crystal habits of the two phases. β -phase crystals form as cubes which facilitates the removal of the wet residue. α -crystals, however, form as dendrites and retain much of the liquid phase. This implies a significant role to be played by the application of the method of the wet residue. The weight per cent H_2O present is listed in table III 3 column 7. This number is an indication of the relative size of the individual particles present in each sample. The average of the weight per cent H_2O present with the α -phase is greater by a factor of 4 as compared to the β -phase.

The second difference in the results of the method of the wet residue for the two phases arises from a comparison of the mole per cent dissolved salts in the liquid phase to the mole per cent salts in the solid phase (shown in Table III 4). The similarity of these two numbers in the β -phase region indicates a small change in the mole ratio obtained from the $Br^- - I^-$ analysis with that obtained after the application of the method of the wet residue.

The large difference, however, between the mole per cent dissolved salts and the mole per cent salts in the solid phase for the α -crystals implies a larger difference in the mole ratio obtained from analysis and that obtained after application of the method of the wet residue.

B. KI-KBr-H₂O at 94°C

1. Analytical Method

Powder photographs of pure KI and pure KBr were taken. The lattice parameters that were obtained for each pair of lines in the far back reflection region were extrapolated to $\theta=90^\circ$ using the function:^{6,10}

$$f(\theta) = \frac{1}{2} \left(\frac{\cos^2 \theta}{\sin \theta} + \frac{\cos^2 \theta}{\theta} \right) .$$

The values of the lattice parameters that were obtained are shown in table III 8. Also shown for comparison are the values obtained by Swanson and Tatge at the National Bureau of Standards. The agreement between the two sets of data is excellent.

Powder photographs were prepared of the KI-KBr solid solutions that were analyzed chemically for the study at 25°C. The lattice parameters were obtained by extrapolation as mentioned above. The extrapolation, here, however, was over a wide range of angles utilizing pairs of lines in some cases starting at $\theta=30^\circ$. The values of the lattice parameters that were obtained are shown in Table III 9 column 2. The film readings are shown in Appendix II. Column 3 lists the type of solid solution(s) present in each case. The x-ray analysis of these solid solutions was used to calibrate the measured lattice constants with composition. The excellent agreement of the lattice constants for the pure components with reliable published data does not necessarily indicate similar accuracy was obtained for the solid solutions. The accuracy obtained is difficult to estimate. The precision, however, is estimated to be within $\pm .002 \text{ \AA}$.

A linear relationship was found to represent the variation of the experimentally obtained lattice parameters with mole per cent KI in the

TABLE III 8

Lattice parameters at room temperature for
pure components

	Present Work, Å	N. B. S., Å (at 25°C) ¹¹
KBr	6.600	6.6000
KI	7.066	7.0655

TABLE III (9)

Calibration of X-ray data

<u>1</u>	<u>2</u>	<u>3</u>	<u>4</u>		<u>5</u>	<u>6</u>
	<u>lattice parameter, A</u>	<u>crystal</u>	<u>Mole Percent KI by chemical analysis</u>		<u>Mole Percent KI by x-ray analysis</u>	<u>Column 4 Column 5</u>
				<u>±</u>		
A	7.066	pure KI	--	--	--	--
B	7.016	β-phase	88.6	.0	88.7	-.1
C	7.016	β-phase	88.0	.2	88.7	-.7
D	6.993	β-phase	83.7	.1	83.5	+ .2
E	6.988	β-phase	82.8	.1	82.4	+ .4
F	6.986	β-phase	82.5	.2	81.9	+ .6
G	6.985	non-equilibrium β-phase	82.1	.2	81.7	--
H	6.986	α+β-phases	81.6	.0	81.9	--
I	6.974	non-equilibrium β-phase	80.2	.0	79.2	--
J	-----	metastable β-phase	80.3	.0	---	--
K	6.976	metastable β-phase	79.8	.0	79.6	+ .2
L	6.984	non-equilibrium β-phase	80.1	.0	81.4	--
M	6.968	metastable β-phase	77.8	.0	77.8	0.0
N	6.987 6.663	α+β-phases	44.6	.2	82.4 14.0	-- --
O	6.657	α-phase	12.8	.2	12.7	+ .1
P	6.651	α-phase	11.6	.1	11.3	+ .3
Q	6.648	α-phase	10.8	.4	10.7	+ .1
R	6.650	α-phase	10.8	.3	11.1	- .3

continued on next page...

TABLE III (9) (cont.)

Calibration of X-ray data

	<u>lattice parameter, A</u>	<u>crystal</u>	<u>Mole Percent KI by chemical analysis</u>		<u>Mole percent KI by x-ray analysis</u>	<u>Column 4 Column 5</u>
S	6.642	α -phase	9.4	.3	9.5	-.1
T	6.644	α -phase	9.0	.0	9.8	-.8
U	6.600	pure KBr	---	--	---	--

solid solutions for α -phase crystals. Similarly, a different linear relationship was found to represent the variation of the experimentally obtained lattice parameters with mole per cent KBr in the solid solutions for β -phase crystals. The equation for each case is shown below:

$$\alpha\text{-phase} \quad a=6.600 + (X_{\text{KI}} \cdot .450) \quad (3.1)$$

$$\beta\text{-phase} \quad a=7.066 - (X_{\text{KBr}} \cdot .442) \quad (3.2)$$

The lattice constants shown in table III 9 column 2 were converted to compositions by use of the above two equations. These compositions are shown in table III 9 column 5. The difference in composition obtained by the chemical analysis compared to the x-ray analysis is shown in column 6. The average of the deviations shown in column 6 is found to $\pm .4$ mole per cent. Reflected in this number is the uncertainty that is present in both the x-ray and the chemical analysis.

Equations 3.1 and 3.2 were used to determine the compositions of the solid solutions prepared by the method of isothermal evaporation at 94°C .

2. Results of Analyses

The data obtained for the system KI-KBr- H_2O at 94°C are shown in table III 10. Columns 2 and 3 list the mole per cent dissolved salts in solution. Column 6 lists the measured lattice parameter for the solid solution obtained at room temperature. Columns 4 and 5 list the mole per cent of each component present in the solid solutions.

The compositions of the solid solutions present in complexes labelled A through D were calculated by use of equation (3.1). The compositions of the solid solutions present in complexes labelled E through F were calculated using equation (3.2).

TABLE III (10)

Mole percent dissolved salts, composition of the solid phase, and
lattice parameter (x-rayed at room temperature) for

KI-KBr-H₂O at 94°C

<u>1</u>	<u>Mole percent dissolved salts in liquid phase</u>		<u>Mole percent salts in solid phase</u>		<u>Lattice parameter \AA</u>
	<u>2</u> <u>KI</u>	<u>3</u> <u>KBr</u>	<u>4</u> <u>KI</u>	<u>5</u> <u>KBr</u>	
A	50.0	50.0	6	94	6.625
B	60.0	40.0	10	90	6.644
C	65.0	35.0	15	85	6.663
D	68.0	32.0	20	80	6.692
E	75.0	25.0	73	27	6.948
F	80.0	20.0	83	17	6.990
G	83.3	16.7	86	14	7.005
H	90.0	10.0	93	7	7.035
I	95.0	5.0	97	3	7.053

The extrapolation of the function

$$f(\theta) = \frac{1}{2} \left(\frac{\cos^2 \theta}{\sin \theta} + \frac{\cos^2 \theta}{\theta} \right)$$

to $\theta=90^\circ$ was over a wide range of angles. In one case, labelled D in table III 10, no sharp pairs of back reflection lines were obtained. In this case, an average value for the film diameter was assumed and the lattice parameter was calculated by use of eight lines from $\theta=11.6^\circ$ to $\theta=34.3^\circ$.

The quality of the film improved as the mole per cent of one of the components present in the solid phase approached 100 percent. For example, the lattice parameter for the solid present in complex labelled H was determined with the use of 9 pairs of back reflection lines. The number of pairs of back reflection lines obtained varied from none for complex D, 3 for complex E, 5 for complex F, 6 for complex G, etc., and similarly for the high KBr solid solutions.

In preliminary experiments, an effort was made to obtain powder photographs of homogeneous solid solutions of compositions approximately 50 mole per cent KI. Liquid solutions with a mole ratio of dissolved salts from 70 to 74 mole per cent KI all yielded solids with lattice parameters corresponding to two different solid phases. The lines obtained on these films were not sharp and often lacked back reflections. This was attributed to phase separation occurring at room temperature. Shown below are several of the pairs of the lattice parameters obtained for the phases found. Also shown are the compositions corresponding to these lattice parameters calculated from equations (3.1) and (3.2).

<u>Lattice Parameter, Å</u>		<u>Mole per cent KI</u>	
6.702	6.880	23	58
6.707	6.930	24	69
6.705	6.940	23	72

The uncertainty in these three sets of parameters is estimated at $\pm 0.010\text{Å}$.

C. KI-NH₄I-third component at 25°C

1. Analytical method

The KI-NH₄I mole ratios were determined by driving off the NH₄I at 500°C. Several mixtures of known amounts of KI and NH₄I were analyzed to test the analytical procedure. These mixtures were prepared both damp and dry. The results were always within $\pm .08$ mole per cent of the true value. This analysis of mixtures, however, does not necessarily indicate that similar accuracy is obtained when the sample analyzed is a solid solution.

A solid solution prepared and analyzed previously in this laboratory by two independent methods⁵ was reanalyzed in duplicate by the method described above. The values of 22.00 and 22.07 weight per cent KI were found for the analyses in the present study. The value of 22.1 weight per cent KI was found in the earlier study by both volumetric and sublimation methods.

2. Results of analyses

The third component employed in the present study contained less than .2 weight per cent dissolved (NH₂OH)₂.H₂SO₄ and NaOH in water. The addition to the H₂O of these substances was necessary to prevent the rapid discoloration of the NH₄I in water. The small amount of these substances added to the H₂O to form the third component was considered to have a negligible effect on the equilibrium between the liquid and solid phases studied.¹²

The data obtained for the system KI-NH₄I-H₂O at 25°C are shown in table III 11. Columns 1, 2, and 3 list the weight in grams of H₂O, NH₄I, and KI that was mixed together initially. Column 8 lists the salt which was added last to the complex. Column 4 contains the weight in grams of the solid phase and the wet residue that was collected from the complex after the complex had reached equilibrium. Column 5 lists the weight per cent salt that was

TABLE III (11)

<u>Experimental Results for NH₄I-KI-H₂O at 25° C</u>										
	<u>1</u> Composition of the <u>2</u> complex in grams		<u>3</u> <u>KI</u>	<u>4</u> Weight Solid Phase and Wet Residue in gms.	<u>5</u> Weight % Salts in Col. 4 <u>+</u>		<u>6</u> Solid and Wet Residue <u>7</u>			<u>8</u> Direction
	<u>H₂O</u>	<u>NH₄I</u>			<u>KI</u>	<u>KI</u>	<u>NH₄I</u>	<u>+</u>		
A	200.00	100.40	258.48	49.70	95.63	.10	80.84	19.16	.00	NH ₄ I
B	200.00	100.40	258.48	48.73	96.23	.21	81.05	18.95	.02	KI
C	200.00	139.92	219.09	38.04	97.34	.01	70.92	29.08	.01	NH ₄ I
D	200.00	139.92	219.09	38.75	96.87	.05	70.59	29.41	.01	KI
E	200.00	169.90	189.09	31.54	95.80	.14	61.58	38.42	.04	NH ₄ I
F	200.00	169.91	189.11	32.55	96.55	.22	61.68	38.32	.06	KI
G	240.00	241.38	197.39	43.39	97.16	.02	52.56	47.38	.00	KI
H	240.00	241.37	197.38	43.72	96.48	.10	52.40	47.60	.02	NH ₄ I
I	150.00	178.28	105.21	33.31	96.97	.05	42.33	57.67	.01	KI
J	150.00	178.78	105.02	34.15	97.31	.06	42.31	57.69	.04	NH ₄ I
K	150.00	187.79	87.85	22.70	97.51	.06	36.24	63.76	.01	KI
L	150.00	197.78	87.79	32.14	96.86	.19	34.81	65.19	.02	NH ₄ I
M	150.00	213.15	64.52	22.28	97.20	.07	25.86	74.14	.02	KI
N	150.00	213.15	64.52	22.65	96.90	.13	25.66	74.34	.03	NH ₄ I

found to be present in the combined solid phase and wet residue. Also shown is the average deviation for this analysis. Column 6 and 7 list the results of the analysis of the salts in the solid phase and the wet residue. Shown also is the average deviation for each of these analyses.

Table III 12 contains the weight per cent of the components present in each phase calculated from the data in table III 11. Column 1 lists the weight per cent salt present in the saturated solution at equilibrium. Columns 2 and 3 list the weight per cent of the dissolved salts present in the aqueous liquid phase. Columns 4 and 5 list the weight per cent of each of the salts present in the solid phase. Comparison of columns 6 and 7 in table III 11 with columns 4 and 5 in table III 12 demonstrate the effect of the wet residue on the composition of the solid phase analysis. This effect can be seen to decrease toward higher weight ratios of NH_4I as the ratio of dissolved salts in the liquid phase approaches the ratio of the salts in the solid phase.

Table III 13 lists the mole per cent dissolved salts in the liquid phase in columns 1 and 2 and the mole per cent salts present in the solid phase in columns 3 and 4.

The indirect method employed in the study of this system to determine the solubilities of the two salts by means of a mass balance calculation is justified by the excellent agreement between the mass balance calculations on the KI-KBr system with the direct experimental results. Further, it can be seen in table III 11 that complexes prepared in duplicate gross compositions (A and B, C and D, E and F, G and H, and M and N) show in table III 12 column 1 good agreement in the weight per cent salt determined to be present in the saturated solutions.

TABLE III (12)

NH₄I-KI-H₂O at 25°C in Weight Per Cent

	<u>1</u>	<u>2</u>	<u>3</u>	<u>4</u>	<u>5</u>	<u>6</u>
	Weight % Salt in Saturated Solution	Weight %		Weight %		Direction
		<u>Dissolved Salts</u>		<u>Solid Phase</u>		
		KI	NH ₄ I	KI	NH ₄ I	
A	61.16	70.67	29.33	81.72	18.28	KI
B	61.15	70.68	29.32	81.62	18.38	NH ₄ I
C	61.80	59.89	40.11	71.41	28.59	NH ₄ I
D	61.79	59.91	40.09	71.19	28.81	KI
E	62.33	51.85	48.15	62.34	37.66	NH ₄ I
F	62.22	51.81	48.19	62.32	37.68	KI
G	62.42	44.18	55.82	53.04	46.96	KI
H	62.45	44.20	55.80	52.93	47.07	NH ₄ I
I	62.77	36.44	63.56	42.65	57.35	KI
J	62.70	36.30	63.70	42.61	57.39	NH ₄ I
K	62.92	31.49	68.51	36.44	63.56	KI
L	63.07	30.24	69.76	35.09	64.91	NH ₄ I
M	63.15	23.01	76.99	26.02	73.98	KI
N	63.14	23.03	76.97	25.78	74.22	NH ₄ I

TABLE III 13NH₄I-KI-H₂O at 25°C in mole per cents

	Mole per cent dissolved Salts in liquid phase		Mole per cent Salts in Solid phase	
	1 <u>KI</u>	2 <u>NH₄I</u>	3 <u>KI</u>	4 <u>NH₄I</u>
A	67.78	32.22	79.60	20.40
B	67.79	32.21	79.50	20.50
C	56.59	43.41	68.56	31.44
D	56.61	43.39	68.33	31.67
E	48.46	51.54	59.10	40.90
F	48.42	51.58	59.08	40.92
G	40.86	59.14	49.65	50.35
H	40.88	59.12	49.54	50.46
I	33.36	66.64	39.37	60.63
J	33.22	66.78	39.33	60.67
K	28.64	71.36	33.36	66.64
L	27.46	72.54	32.06	67.94
M	20.69	79.31	23.49	76.51
N	20.71	79.29	23.27	76.73

The complexes labelled I and J turned faintly yellow after 12 days with continual stirring and grinding. The stirring was then stopped at this time and the complexes were analyzed. In all of the other complexes the solution remained clear and free of discoloration. Crystals obtained in all of the cases, including complexes I and J, were white and exhibited faces that were shiny.

Shown in Table III 15 are the data obtained in the determination of the solubility of pure NH_4I at 25°C in the solvent employed in the present study. Columns one and two list the weight in grams of H_2O and NH_4I that was used to prepare the complex. Column three lists the combined weight of the solid phase and the wet residue found experimentally. Column four lists the weight per cent salt determined experimentally to be present in the solid phase and wet residue. Column five lists the solubility expressed as weight per cent NH_4I present in the saturated solution. Column six lists the solubility expressed as the molality NH_4I .

The excellent agreement between the two determinations confirms the attainment of equilibrium within the limits of error of the experiment.

Powder photographs were taken of pure KI (as already described in section III B) and of pure NH_4I . The values of the lattice parameters obtained are shown in table III 14. KI is shown here again for completeness. For comparison, the values obtained by Swanson, Fuyat and Urginic at the N. B. S. are also shown. The agreement is excellent.

Powder photographs were taken of the solid solutions labelled G and I in table III 13. Shown in table III 14 are the values of the lattice parameters obtained for these crystals. The values of θ , $f(\theta)$, d , and a for the lines used in the extrapolation to obtain a at $\theta=90^\circ$ are given in Appendix II.

The powder photographs of the solid solutions were of high quality with α, α_2 doublet separation in the back reflection region. The films of the pure components were sharper than those of the solid solutions. Higher back reflection lines were also present on the films of the pure components than were present on the films of the solid solutions.

The excellent agreement between the lattice parameters obtained at the N. B. S. and the present data for the pure components does not necessarily imply similar accuracy was obtained for the solid solutions. The precision obtained for the powder pattern determination of the lattice parameters is estimated at $\pm .002 \text{ \AA}$.

TABLE III (14)

Lattice Parameters at Room Temperature for Pure Components and
Solid Solutions of KI-NH₄I

	Present Study (Å)	N. B. S. (Å)
<u>Pure Components</u>		
KI	7.066	7.0655 (at 25°C) ¹¹
NH ₄ I	7.261	7.2613 (at 26°C) ¹³
<u>Solid Solutions</u>		
50.35 mole per cent NH ₄ I (G)	7.168	
50.46 mole per cent NH ₄ I (H)	7.168	

TABLE III 15

Solubility Determination of Pure NH₄I at 25°C

1	2	3	4	5	6
Composition of the Complex in grams		Weight Solid Phase and Wet Residue in grams	Weight % Salt in Col. 3	Weight % Salt in saturated solution	Molality NH ₄ I
H ₂ O	NH ₄ I				
<u>From undersaturation (5 days)</u>					
150.00	307.19	49.78	96.86 ± .05	63.56	12.03
<u>From oversaturation (3 days)</u>					
150.00	307.27	49.87	97.13 ± .02	63.53	12.02

CHAPTER IV DISCUSSION

A. KI-KBr and KI-KBr-H₂O at 25°C

The miscibility gap in the system KI-KBr has been studied by a variety of methods by several groups¹⁴⁻²⁴. In none of these studies, however, has the attainment of equilibrium with respect to changes in the composition of a macroscopic solid phase been demonstrated. The limits of error in the experimental data in most cases are too large to be useful for extracting thermodynamic information. In the other cases, upon analysis, the data are found to be thermodynamically inconsistent by the methods discussed in section I.

The data obtained in the present study for the solid solutions of KI-KBr at 25°C shown in tables III (3) and III (4) were analyzed by two independent thermodynamic paths.

An important step in the thermodynamic analysis of this system is a knowledge of the composition of the limiting crystals at the miscibility gap. Solid solutions labelled F and O in table III (3) and III (4) were prepared by the method of the infinitesimal approach to the limiting miscibility. As discussed in section II, a liquid solution of the saturated three component isothermally invariant composition had added to it small amounts of solid KI (beaker F) or solid KBr (beaker O). After several weeks stirring to achieve equilibrium between the liquid and solid solutions, the crystals obtained in each case were of a single phase. The fact that these were in a single phase region was insured by the method of preparation of the complexes. Thus, the compositions of these two solid solutions, assuming equilibrium was achieved with respect to composition in the solid phase within the limits of the experimental accuracy, puts limits on the possible width of the miscibility

gap at 25°C. Comparison of the compositions of the liquid solutions of these two complexes with that of a solution saturated with both α and β solid solutions (complex N) indicates how close complexes F and O are to that of the limiting miscibility. As can be seen from table III (4), the experimental data for the liquid solutions N and O overlap each other within the exceptionally small limits of error obtained for these two solutions.

The short extrapolations to the composition of the solid solutions of the limiting miscibility on both sides of the miscibility gap were performed using the following functions:

$$K'_{KI} = \frac{m_{K^+} m_{I^-}}{X_{KI}} \quad , \quad K'_{KBr} = \frac{m_{K^+} m_{Br^-}}{X_{KBr}} \quad . \quad (4.1,2)$$

The experimental values of K'_{KBr} and K'_{KI} were plotted as functions of m_{KI} and m_{KBr} and extrapolated to the value of the isothermally invariant solution. For the composition of the isothermally invariant solution, the average was taken of the values of the best analyses of this three-component solution. This average value is the following:

$$7.293 \text{ molal KI} \quad , \quad 2.309 \text{ molal KBr} \quad .$$

This corresponds to the following mole fractions of dissolved salts in the liquid phase:

$$.7595 \text{ mole KI} \quad , \quad .2405 \text{ mole KBr} \quad .$$

The values obtained for the miscibility gap for the system KI-KBr at 25°C with maximum limits of error estimated are the following:

$$\begin{array}{ll} \alpha\text{-phase} & 12.70 \pm .30 \text{ mole per cent KI} \\ \beta\text{-phase} & 82.20 \pm .20 \text{ mole per cent KI} \end{array} \quad .$$

The composition of the limiting miscibility being known allows the free energy parameters B_g and C_g to be evaluated from equations (1.25)

and (1.26). The values of B_g and C_g obtained by this method are the following at 25°C:

$$B_g = 2.4645$$

$$C_g = -.1505$$

The values of the activity coefficients for the two-component system KI-H₂O⁹ and KBr-H₂O^{8,25} at 25°C have been determined experimentally as a function of molality. This enables a more detailed study of the equilibrium involved in the KI-KBr-H₂O three-component system than is generally possible.

The equilibrium constants of interest are the following:

$$K_1 = \frac{(\gamma_{1\pm})^2 m_{K^+} m_{I^-}}{f_1 X_1} \quad (4.3)$$

$$K_2 = \frac{(\gamma_{2\pm})^2 m_{K^+} m_{Br^-}}{f_2 X_2} \quad (4.4)$$

Equations (3) and (4) are equations (1) and (2) with activity coefficients included. γ_1 and γ_2 are the mean activity coefficients of KI and KBr respectively in the three-component KI-KBr-H₂O system.

$\gamma_1(0)$ and $\gamma_2(0)$ represent the mean activity coefficients of KI and KBr in their respective two-component salt-H₂O systems. It can be seen that when $X_1 = 1$, $\gamma_1 = \gamma_1(0)$ and similarly when $X_2 = 1$, $\gamma_2 = \gamma_2(0)$.

At this point, equations (3) and (4) are evaluated in order to obtain values of K_1 and K_2 . For the two-component systems KI-H₂O and KBr-H₂O, m_{I^-} and m_{Br^-} have been measured at saturation. f_1 and f_2 are equal to unity for the pure components X_1 and X_2 respectively. $\gamma_1(0)$ and $\gamma_2(0)$ have been measured^{9,8}. Thus, the values of the constants K_1 and K_2 are found to be

$$K_1 = 55.94 \quad \text{and} \quad K_2 = 13.42 \quad .$$

f_1 is known as a function of X_1 and f_2 is known as a function of X_2 (see 1.15 and 1.16). Therefore, the activity coefficients γ_1 and γ_2 can be computed for the experimental points by using equations (3) and (4). Shown in table IV (1) parts (a) and (b) are the experimentally determined values of the activity coefficients for the liquid and solid phases for the KI-KBr-H₂O system. By reference to this table, γ_1 and γ_2 can be seen to vary only slightly over the range of total molalities involved in the present study. These small variations, however, can be represented over the range of the experimental data as functions of m_T , m_1 , and m_2 . The values of $\log \gamma_{1(0)}$ and $\log \gamma_{2(0)}$ for the two-component systems are required for this representation in the range of total molalities of the data of the three-component system. The system KI-KBr-H₂O at 25°C, however, belongs to the Roozeboom type IV²⁶ class of systems. This group of three-component systems contain an isothermal invariant liquid solution of three-components at the minimum vapor pressure of the saturated liquid phase. This implies, for the present system, that part of the range of total molalities of the three-component liquid solution will have a higher total molality than that of either of the two separate two-component liquid solutions. Thus, direct experimental determination of $\log \gamma_{1(0)}$ and $\log \gamma_{2(0)}$ in the range of total molalities near that of the isothermally invariant solution is not possible.

This difficulty is overcome by extrapolating the data in the region where activity coefficients are experimentally available to higher molalities corresponding to supersaturated two-component solutions.

Expressions representing $\log \gamma_{1(0)}$ and $\log \gamma_{2(0)}$ derived for this purpose are shown:

$$\log \gamma_{1(0)} = .01949(m_T - 5.50) - .1457 \quad (4.5)$$

TABLE IV (1) Part (a)

KI-KBr-H₂O at 25°C

Experimental Values of Activity Coefficients in Liquid
and Solid Phases

	x_1^s	m_1	m_2	γ_1	γ_2	$\log \frac{\gamma_1^2}{\gamma_2}$
<u>β-Phase</u>						
B	.8858	7.633	1.856	.8384	.7513	.0954
C	.8797	7.611	1.886	.8377	.7559	.0892
D	.8371	7.369	2.215	.8374	.7471	.0991
E	.8285	7.338	2.247	.8374	.7494	.0965
F	.8248	7.302	2.298	.8381	.7434	.1041
<u>Metastable Phase</u>						
J	.8030	7.291	2.319	.8345	.7546	.0874
K	.7985	7.278	2.343	.8341	.7528	.0890
M	.7780	7.222	2.410	.8339	.7514	.0905
<u>α-Phase</u>						
O	.1278	7.286	2.316	.8394	.7425	.1065
P	.1158	7.247	2.323	.8266	.7447	.0907
Q	.1080	7.034	2.411	.8317	.7372	.1047
R	.1082	7.003	2.424	.8346	.7359	.1094
S	.0942	6.716	2.511	.8329	.7336	.1103
T	.0896	6.662	2.551	.8259	.7293	.1080

TABLE IV (1) Part (b)

KI-KBr-H₂O at 25°C

Experimental Values of Activity Coefficients in Liquid
and Solid Phases

	x_1^s	f_1	f_2	log D
<u>β-Phase</u>				
B	.8858	1.0275	6.4857	-.2753
C	.8797	1.0306	6.3394	-.2582
D	.8371	1.0576	5.4207	-.1888
E	.8285	1.0642	5.2552	-.1700
F	.8248	1.0672	5.1860	-.1708
<u>Metastable Phase</u>				
J	.8030	1.0862	4.7994	-.1127
K	.7985	1.0905	4.7245	-.1054
M	.7780	1.1116	4.3996	-.0680
<u>α-Phase</u>				
O	.1278	6.8949	1.0475	1.3321
P	.1158	7.3150	1.0389	1.3768
Q	.1080	7.6059	1.0338	1.3816
R	.1082	7.5983	1.0339	1.1377
S	.0942	8.1581	1.0257	1.4101
T	.0896	8.3535	1.0232	1.4241

$$\log \gamma_2(0) = .01408(m_T - 4.50) - .2104 \quad (4.6)$$

The experimental activity coefficients in the three-component liquid solutions are represented in the following form^{25,27}:

$$\log \gamma_1 = \log \gamma_1(0) - \alpha_1 m_2 \quad (4.7)$$

$$\log \gamma_2 = \log \gamma_2(0) + \alpha_2 m_1 \quad (4.8)$$

For the experimental data points, $\log \gamma_1$, $\log \gamma_1(0)$ and m_2 are known.

This enables α_1 to be evaluated. Similarly, α_2 can be evaluated.

The functional relationships for α_1 and α_2 obtained are shown:

$$\alpha_1 = .00533(m_T - 9.20) + .0029 \quad (4.9)$$

$$\alpha_2 = .00114(m_1 - 7.00) + .0012 \quad (4.10)$$

Substitution of equations (9) and (10) into equations (7) and (8), respectively, leads to the following equations:

$$\log \gamma_1 = \log \gamma_1(0) - [.00533(m_T - 9.20) + .0029]m_2 \quad (4.11)$$

$$\log \gamma_2 = \log \gamma_2(0) + [.00114(m_1 - 7.00) + .0012]m_1 \quad (4.12)$$

The logarithms of the experimentally obtained activity coefficients are compared with those obtained from the above expressions in tables IV (2) and IV (3). The agreement is excellent. Equations (11) and (12) are valid for only total molalities in the region of the experimental data.

Thus, inspection of equations (3) and (4) now reveals that for an arbitrary value of X_1 in the solid phase, these two equations can be solved for the composition of the three-component liquid phase.

f_1 and f_2 are known as functions of X_1 and X_2 by equations (1.15) and (1.16). γ_1 and γ_2 are known as functions of m_1 , m_2 and m_T through equations (4.11) and (4.12). The constants K_1 and K_2 are known. The only restrictions upon evaluating (3) and (4) is that γ_1 and γ_2 are

TABLE IV (2)

KI-KBr-H₂O at 25°C

log γ_2

Experimental and Calculated Values

$$\log \gamma_{2(0)} = .01408(m_T - 4.50) - .2104$$

$$\log \gamma_2 = \log \gamma_{2(0)} + [.00114(m_1 - 7.00) + .0012]m_1$$

	Experimental	Calculated	Experimental minus Calculated
<u>β-Phase</u>			
B	-.1242	-.1255	+0.0013
C	-.1215	-.1256	+0.0041
D	-.1266	-.1269	+0.0003
E	-.1253	-.1272	+0.0019
F	-.1288	-.1273	-.0015
<u>Metastable Phase</u>			
J	-.1223	-.1273	+0.0050
K	-.1233	-.1273	+0.0040
M	-.1241	-.1277	+0.0036
<u>α-Phase</u>			
O	-.1293	-.1275	-.0018
P	-.1280	-.1283	+0.0003
Q	-.1324	-.1321	-.0003
R	-.1332	-.1327	-.0005
S	-.1346	-.1358	+0.0012
T	-.1371	-.1365	-.0006

TABLE IV (3)

KI-KBr-H₂O at 25°C

log γ_1

Experimental and Calculated Values

$$\log \gamma_1(0) = .01949(m_T - 5.50) - .1457$$

$$\log \gamma_1 = \log \gamma_1(0) - [.00533(m_T - 9.20) + .0029]m_2$$

	Experimental	Calculated	Experimental minus Calculated
<u>β-Phase</u>			
B	-.0765	-.0762	-.0003
C	-.0769	-.0762	-.0007
D	-.0771	-.0771	.0000
E	-.0771	-.0772	+.0001
F	-.0767	-.0774	+.0007
<u>Metastable Phase</u>			
J	-.0786	-.0774	-.0012
K	-.0788	-.0774	-.0014
M	-.0789	-.0777	-.0012
<u>α-Phase</u>			
O	-.0760	-.0775	+.0015
P	-.0827	-.0777	-.0050
Q	-.0801	-.0789	-.0012
R	-.0785	-.0789	+.0004
S	-.0794	-.0807	+.0013
T	-.0831	-.0809	-.0022

known only in the region of the experimental data of the total molalities. This corresponds to the requirement that x_1 is restricted to the following values when evaluating equations (3) and (4):

$$.09 \leq x_1 \leq .95$$

Shown in table IV (4) are the experimental and the calculated values of the molality of KI in the liquid phase for each experimentally determined mole fraction of KI in the solid phase. Table IV (5) similarly lists the experimental and the calculated values of the molality of KBr in the liquid phase for each of the experimentally determined pairs of solid-liquid equilibrium points. Also, table IV (6) lists the experimental and the calculated values of the weight per cent salt dissolved in the saturated solutions. In each of these tables, the difference between the experimental and the calculated values is shown.

Inspection of table IV (2) through IV (6) reveals that the best agreement is found for $\log \gamma_1$ and m_1 for mixtures containing β -phase solid solutions, and also for $\log \gamma_2$ and m_2 for mixtures containing α -phase solid solutions. The agreement in the region of the metastable solid solutions is not as good as that in the region of the stable phase solid solutions. This last fact is expected considering that the experimental method involved isothermal relief of supersaturation.

Shown in Appendix III are the calculated compositions for the KI-KBr-H₂O system employing equations (3) and (4).

The free energy parameters E_g and C_g evaluated from the equilibrium between two solid solutions have the same values as that needed to represent the data within the limits of experimental accuracy for the equilibrium between a solid and its saturated aqueous phase. Thus, by considering these two equilibria as expressed by equations (1.18) and (1.19) and by (1.29), the present data meet the thermodynamic

TABLE IV (4)

KI-KBr-H₂O at 25°CExperimental and Calculated Molalities of KI

	X_1^B	m_1 Experimental	m_1 Calculated	Experimental minus Calculated
<u>β-Phase</u>				
B	.8858	7.633	7.622	+0.011
C	.8797	7.611	7.584	+0.027
D	.8371	7.369	7.368	+0.001
E	.8285	7.338	7.334	+0.004
F	.8248	7.302	7.320	-.018
<u>Metastable Phase</u>				
J	.8030	7.291	7.249	+0.042
K	.7985	7.278	7.236	+0.042
M	.7780	7.222	7.186	+0.036
<u>α-Phase</u>				
O	.1278	7.286	7.321	-.035
P	.1158	7.247	7.148	+0.099
Q	.1080	7.034	7.014	+0.020
R	.1082	7.003	7.018	-.015
S	.0942	6.716	6.727	-.011
T	.0896	6.662	6.614	+0.048

TABLE IV (5)

KI-KBr-H₂O at 25°CExperimental and Calculated Molalities of KBr

	X_1^B	m_2 Experimental	m_2 Calculated	Experimental minus Calculated
<u>β-Phase</u>				
B	.8858	1.856	1.868	-.012
C	.8797	1.886	1.922	-.036
D	.8371	2.215	2.217	-.002
E	.8285	2.247	2.263	-.016
F	.8248	2.298	2.281	+.017
<u>Metastable Phase</u>				
J	.8030	2.319	2.373	-.054
K	.7985	2.343	2.389	-.046
M	.7780	2.410	2.451	-.041
<u>α-Phase</u>				
O	.1278	2.316	2.290	+.026
P	.1158	2.323	2.360	-.037
Q	.1080	2.411	2.416	-.005
R	.1082	2.424	2.414	+.010
S	.0942	2.511	2.535	-.024
T	.0896	2.551	2.582	-.031

TABLE IV (6)

KI-KBr-H₂O at 25°CExperimental and Calculated Weight Per Cent Salts
in Saturated Solution

	x_1^g	Weight Per Cent Salts		Experimental minus Calculated
		Experimental	Calculated	
<u>β-Phase</u>				
B	.8858	59.81	59.80	+ .01
C	.8797	59.82	59.80	+ .02
D	.8371	59.79	59.79	.00
E	.8285	59.77	59.79	- .02
F	.8248	59.77	59.79	- .02
<u>Metastable Phase</u>				
J	.8030	59.78	59.77	+ .01
K	.7985	59.79	59.77	+ .02
M	.7780	59.77	59.75	+ .02
<u>α-Phase</u>				
O	.1278	59.76	59.80	- .04
P	.1158	59.67	59.47	+ .20
Q	.1080	59.26	59.21	+ .05
R	.1082	59.20	59.22	- .02
S	.0942	58.57	58.65	- .08
T	.0896	58.50	58.43	+ .07

criteria of yielding a free energy of mixing that is independent of path.

The equations that were derived for the activity coefficients in the aqueous phase are valid only in the range of the experimental data. At this point, equations are derived that are valid over the whole range of compositions using the assumption that the $\log \frac{\gamma_1^2}{\gamma_2^2}$ term in equation (1.33) is a constant. This term is not strictly a constant and varies as a different linear function of m_T on each side of the miscibility gap. The experimental points can be represented to approximately the limits of the experimental accuracy assuming this term a constant. A comparison of the experimental data with the calculated values is shown in table IV (7). This is shown in figure 1. Appendix IV contains the calculated values throughout the whole range of mole fractions in the solid phase. The activity coefficients are not known throughout the whole range of compositions in the liquid phase so that molalities cannot be calculated from equation (1.33). The log D term is evaluated in terms of mole fractions as shown by equation (1.34).

Shown in Appendix V are the values of the free energy of mixing for the KI-KBr system at 25°C calculated from equation (1.3) using the B_g and C_g values derived in this section. Shown in Appendix VI are the values of the activities of X_1 and X_2 , a_1 and a_2 respectively, obtained from equations (1.13) through (1.16).

Notice that the value of the activity of X_2 goes above unity from approximately $.60 < X_1 < .75$. If the metastable branch of the log D curve were studied at 25°C, this portion of the curve would be experimentally inaccessible.

The following should be noted concerning the preparation of solid solutions. Complexes labelled G, L, and I are not of thermodynamic

TABLE IV (7)
KI-KBr - H₂O at 25°C

Comparison of Experimental and Calculated Mole Fractions of Dissolved Salts in Aqueous Phase Calculated by

Method I:	<u>Two Methods</u>		Method II:			
$\log \frac{\gamma_1^2}{\gamma_2} = \text{function of } m_1 \text{ and } m_2$			$\log \frac{\gamma_1^2}{\gamma_2} = \text{constant}$			
<u>X₁^s</u>	<u>X₁^l Experimental</u>	<u>X₁^l Calculated Method I</u>	<u>X₁^l Calculated Method II</u>	<u>Experimental- Calculated Method I</u>	<u>Experimental- Calculated Method II</u>	
<u>β-Phase</u>						
B	.8858	.8045	.8032	.8023	+ .0013	+ .0022
C	.8797	.8014	.7978	.7970	+ .0036	+ .0044
D	.8371	.7689	.7687	.7680	+ .0002	+ .0009
E	.8285	.7656	.7642	.7636	+ .0014	+ .0020
F	.8248	.7606	.7625	.7618	- .0019	- .0012
<u>Metastable Phase</u>						
J	.8030	.7587	.7534	.7528	+ .0053	+ .0059
K	.7985	.7566	.7518	.7512	+ .0048	+ .0054
M	.7780	.7498	.7456	.7451	+ .0042	+ .0047
<u>α-Phase</u>						
O	.1278	.7589	.7618	.7609	- .0029	- .0020
P	.1158	.7572	.7517	.7526	+ .0055	+ .0046
Q	.1080	.7446	.7438	.7461	+ .0008	- .0015
R	.1082	.7428	.7441	.7463	- .0013	- .0035
S	.0942	.7278	.7263	.7318	+ .0015	- .0040
T	.0896	.7232	.7193	.7261	+ .0039	- .0029

significance. These data are included to show the effect of stirring on the composition of the solid phase obtained when the method of isothermal relief of supersaturation is employed. Complexes G and I in table III (3) were prepared from the identical supersaturated solution as described in detail in section III. The composition of the solid phases obtained differ by approximately 2 mole per cent. Clearly, stirring in one case and not stirring in the other had a marked effect on the composition of the solid obtained.

The metastable region of solid solutions obtained in the present study can be interpreted in terms of the metastable zone width of the aqueous solutions of KI and of KBr²⁸. It is found that KBr solutions have a larger region of supersaturation than that of KI. In the present study, this can explain the obtaining of KI rich (β -phase) metastable solid solutions without KBr rich (α -phase) solid solutions depositing out of the supersaturated solution.

B. KI-KBr at all temperatures and KI-KBr-H₂O at 94°C

The free energy of mixing for the solid solutions of KI-KBr has been determined at 25°C from the data in the present study. The combination of the expressions obtained at 298°K with expressions derived from reliable literature data at the azeotrope temperature enable all of the thermodynamic properties of interest over a 1000° range to be evaluated. It will be shown that the expressions obtained are consistent with experimental heats of mixing and with the free energy data obtained in the present study at 367°K.

The notation employed in this section is the same as that used in previous sections with the exception that superscripts are used, where needed, to distinguish between parameters for the molten liquid (l) and solid (s) phases.

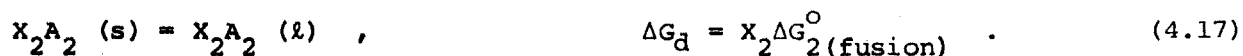
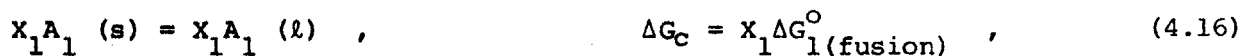
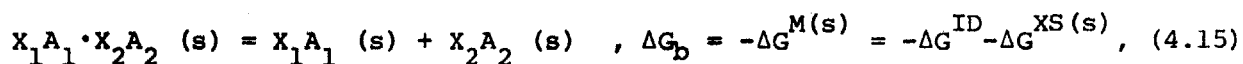
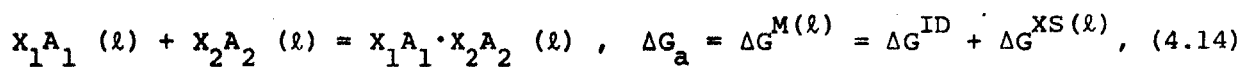
Consider the following change in state:



This represents one mole of a solid solution of composition $X_1A_1 \cdot X_2A_2$ which melts to give a molten liquid of the same composition at constant temperature and pressure. This is found in the KI-KBr system^{29,30,31}, by definition, at the point of the azeotropic composition and temperature. At other temperatures and compositions, this change in state corresponds to a metastable melting point as would occur if unmixing in the solid phase did not take place during the melting process.

The free energy parameters for the molten liquid and solid phases need to be evaluated to enable the behavior of the liquidus and solidus curves to be predicted. Expressions to describe the solid-liquid equilibrium are derived by two methods. The first method is restricted to the metastable melting points and azeotropic behavior. It is a useful aid in understanding the equilibria involved. The second method is general in application and will be shown to lead to the same expression as that of the first method when applied under restricted conditions.

Consider the following changes in state at a constant T and p:



The sum of the changes in state (14) through (17) is given by

$$X_1 A_1 \cdot X_2 A_2 (s) = X_1 A_1 \cdot X_2 A_2 (l) ,$$

The sum of ΔG_a , ΔG_b , ΔG_c , ΔG_d is shown below:

$$\Delta G_{\text{Total}} = \Delta G^{\text{XS}(l)} - \Delta G^{\text{XS}(s)} + X_1 \Delta G_1^{\circ}(\text{fusion}) + X_2 \Delta G_2^{\circ}(\text{fusion}) \quad (4.18)$$

As stated earlier, the above change in state is for one mole of solid solution melting congruently to give one mole liquid solution at a constant temperature and pressure. This corresponds to the intersection of the free energy of mixing curves for the liquid and solid phases. At the minimum melting temperature, the free energy of mixing of the solid and liquid phases are equal and equation (18) represents the equilibrium change in state. At other temperatures and compositions, the solutions of equation (18) are the metastable melting points of the solid solutions.

Substitution of equations (1.2) and (1.3) into equation (18), and recalling that at the minimum melting temperature and at the metastable melting points,

$$X_1^s = X_1^l , \quad (4.19)$$

$$X_2^s = X_2^l , \quad (4.20)$$

the following is obtained:

$$\frac{\Delta G_1^{\circ}(\text{fusion})}{X_2} + \frac{\Delta G_2^{\circ}(\text{fusion})}{X_1} = RT[(B_g^{(s)} - B_g^{(l)}) + (C_g^{(s)} - C_g^{(l)})(X_1 - X_2)] \quad (4.21)$$

Equation (21) determines the metastable melting point composition when the values of $(B_g^{(s)} - B_g^{(l)})$, $(C_g^{(s)} - C_g^{(l)})$, ΔG_1° and ΔG_2° are known.

Equation (21) can be obtained as a limited case of a more general expression of more practical use. Consider the following equilibria:

$$A_1 (c.s.) = A_1 (l) , \quad (4.22)$$

$$A_2 \text{ (c.s.)} = A_2 \text{ (l)} \quad (4.23)$$

The corresponding equilibrium constants are:

$$K_1 = \frac{a_1^{(l)}}{a_1^{(c.s.)}} = \frac{f_1^{(l)} X_1^{(l)}}{f_2^{(s)} X_1^{(s)}} \quad (4.24)$$

and

$$K_2 = \frac{a_2^{(l)}}{a_2^{(c.s.)}} = \frac{f_2^{(l)} X_2^{(l)}}{f_2^{(s)} X_2^{(s)}} \quad (4.25)$$

Taking the logarithm of equations (24) and (25) and using the fact that $\Delta G_1^{\circ} = -RT \ln K_1$, and $\Delta G_2^{\circ} = -RT \ln K_2$, the following two expressions are obtained which are similar in form to equations (1.23) and (1.24):

$$\frac{-\Delta G_1^{\circ}}{RT} = \ln f_1^{(l)} - \ln f_1^{(s)} + \ln \frac{X_1^{(l)}}{X_1^{(s)}} \quad (4.26)$$

$$\frac{-\Delta G_2^{\circ}}{RT} = \ln f_2^{(l)} - \ln f_2^{(s)} + \ln \frac{X_2^{(l)}}{X_2^{(s)}} \quad (4.27)$$

On substitution of equation(1.15)and (1.16) into (26) and (27) above, two useful expressions [which are similar in form to equations (1.25) and (1.26)] are obtained:

$$(X_2^l)^2 [B_g^l + C_g^l(4X_1^l - 1)] - (X_2^s)^2 [B_g^s + C_g^s(4X_1^s - 1)] + \ln \frac{X_1^l}{X_1^s} = \frac{-\Delta G_1^{\circ}}{RT} \quad (4.28)$$

$$(X_1^l)^2 [B_g^l + C_g^l(4X_1^l - 3)] - (X_1^s)^2 [B_g^s + C_g^s(4X_1^s - 3)] + \ln \frac{X_2^l}{X_2^s} = \frac{-\Delta G_2^{\circ}}{RT} \quad (4.29)$$

Thus, these two equations can be used to calculate the liquidus-solidus behavior when the temperature dependent variables B_g^l , C_g^l , B_g^s , and C_g^s have been evaluated and the free energy of fusion of the pure components

is known. Conversely, if the solidus-liquidus behavior is known, the parameters B_g^l , B_h^l , B_s^l and C_g^l , C_h^l , C_s^l can be evaluated from the above two equations and equations (1.4) and (1.5). When the value of these parameters are known, the value of the entropy, enthalpy, and the free energy of mixing at any temperature and composition can be evaluated.

Recall that at the minimum melting temperature of the solid solutions that equations (19) and (20) hold. Substitution of equations (19) and (20) into equations (28) and (29) yields the following useful expressions:

$$(B_g^s - B_g^l) = \frac{\Delta G_1^0}{X_2^2 RT} - (C_g^s - C_g^l)(4X_1 - 1) \quad (4.30)$$

$$(B_g^s - B_g^l) = \frac{\Delta G_2^0}{X_1^2 RT} - (C_g^s - C_g^l)(4X_1 - 3) \quad (4.31)$$

Thus, if the value of the free energy parameters for either the liquid or solid phase are known at the azeotrope temperature and composition, then the two parameters for the other phase can be determined. Notice that equations (30) and (31) reduce to equation (21) at the metastable melting points.

For the KI-KBr system, equations (30) and (31) have been used to determine the values of $(B_g^s - B_g^l)$ and of $(C_g^s - C_g^l)$ from the literature data³¹ at the azeotrope temperature. The following values were obtained at the temperature shown:

$$B_g^s - B_g^l = .52 \quad (T = 937^\circ\text{K}) \quad , \quad (4.32)$$

$$C_g^s - C_g^l = -.05 \quad (T = 937^\circ\text{K}) \quad . \quad (4.33)$$

The free energy parameters in the liquid phase, B_g^l and C_g^l , have been

estimated to be

$$B_g^l = \frac{60}{T} = \frac{60}{937} = .06 \quad , \quad (4.34)$$

$$C_g^l = 0 \quad . \quad (4.35)$$

on the basis of the values obtained for these parameters in other systems of binary alkali halides³².

Equations (32), (33), and (34), (35) are solved for the value of the free energy parameters in the solid phase at the azeotrope temperature. The following values are obtained:

$$B_g^s = .58 \quad (T = 937^\circ\text{K}) \quad , \quad (4.36)$$

$$C_g^s = -.05 \quad (T = 937^\circ\text{K}) \quad . \quad (4.37)$$

Thus, B_s^s , B_h^s , C_s^s , and C_h^s can be evaluated over a temperature range of 639° from literature data at 937°K and from data in the present study at 298°K.

Recall the values of B_g^s and C_g^s obtained at 298.15°K in section A:

$$B_g^s = 2.4645 \quad (T = 298.15^\circ\text{K})$$

$$C_g^s = -.1505 \quad (T = 298.15^\circ\text{K})$$

Thus, the following values are obtained by a combination of the above two values with the values shown in equations (36) and (37):

$$B_g^s = \frac{B_h^s}{T} - B_s^s \quad ; \quad B_h^s = 824.08 \quad , \quad B_s^s = .2995 \quad , \quad (4.38)$$

$$C_g^s = \frac{C_h^s}{T} - C_s^s \quad ; \quad C_h^s = -44.87 \quad , \quad C_s^s = 0 \quad . \quad (4.39)$$

All of the thermodynamic properties of the KI-KBr system from near 0°K to over 1000°K can be evaluated using the parameters shown above in equations (34) through (39). The experimental data obtained in

the present study at 367°K is now compared to that obtained employing these parameters.

Equations (38) and (39) are solved for the free energy parameters in the solid phase, B_g^S and C_g^S , at 367°K. The predicted values are shown below:

$$B_g^S = 1.9450 \quad (\text{at } 367^\circ\text{K}) \quad (4.40)$$

$$C_g^S = -.2222 \quad (\text{at } 367^\circ\text{K}) \quad (4.41)$$

For each experimental point, the value of $\log D$ is calculated using the definition of D shown in equation (1.34) and $\log \frac{f_2}{f_1}$ is calculated using the values of B_g^S and C_g^S shown above substituted into equation (1.35).

This enables the value of $(\log K - \log \frac{\gamma_1^2}{\gamma_2})$ to be obtained for each experimental point by use of equation (1.33). Using the approximation shown to be valid earlier that $\log \frac{\gamma_1^2}{\gamma_2}$ is a constant within the limits of

experimental accuracy, the value of $(\log K - \log \frac{\gamma_1^2}{\gamma_2})$ is then also a

constant. The value of this constant is taken as the average of the values found.

Thus, by use of equations (1.33) and (1.34), the mole fraction in the solid phase in equilibrium with the mole fraction of dissolved salts in the aqueous phase can be calculated. This calculation is performed as a check on the B_g^S and C_g^S parameters shown in equations (4.38) through (4.41), and as a check on the precision of the experiment. Shown in table IV (8) is a comparison of the experimental and calculated values of the mole fraction of dissolved salts in the aqueous phase. Appendix VIII contains the calculated values throughout the whole range of mole fraction

TABLE IV (8)

KI-KBr-H₂O at T = 367°K

Experimental and Calculated Mole Fractions of Dissolved
Salts in Aqueous Liquid Phase

	x_1^s	x_1^l Experimental	x_1^l Calculated	Experimental minus Calculated
A	.6	.50	.52	-.02
B	.10	.60	.62	-.02
C	.15	.65	.67	-.02
D	.20	.68	.70	-.02
E	.73	.75	.76	-.01
F	.83	.80	.80	.00
G	.86	.83	.82	+.01
H	.93	.90	.89	+.01
I	.97	.95	.94	+.01

in the solid phase.

The calculation discussed above was based upon two considerations. The first consideration is the variation of $\log D$ with mole fraction, which is seen by rewriting equation (1.33) in the form

$$\log D = \log K - \log \frac{\gamma_1^2}{\gamma_2} - \log \frac{f_2}{f_1} . \quad (4.42)$$

The only term that is not a constant on the right side of the above equation is the term involving the activity coefficients in the solid phase. This term was calculated from equation (1.35) using the free energy parameters derived from experimental data at 298°K and 937°K. The calculated value of $\partial \log D / \partial X_1$ was not obtained from the actual experimental data at this temperature. The other consideration in the calculation is the constant term. In the absence of data concerning the activity coefficients in the aqueous phase at this temperature, it was necessary to supply the constant in equation (42) from the present data by the means described.

A plot of $\log D$ as a function of mole fraction in the solid phase at 367°K is shown in figure 2. The estimated error bars correspond to ± 1 mole per cent in the solid phase. The agreement between the experimental and calculated values must be considered good for data obtained at this temperature.

The slope of this $\log D$ curve demonstrates that this temperature is above the critical mixing temperature for the appearance of two solid phases. This can be seen by observing the change in the calculated composition of the homogeneous solid phase with the change in the composition of the saturated aqueous phase shown in Appendix VII. The mole fraction of KI rises continuously both in the aqueous liquid and and solid phases.

The fact that data points were not obtained for homogeneous solid solutions throughout the whole range of mole fractions in the solid phase is due to the rapid decomposition of the homogeneous solid solutions at room temperature into two phases. The decomposition took place during the period of time necessary to obtain powder photographs of the samples at room temperature (see section II and III). It is known that moisture acts as a catalyst for this phase change¹⁹.

The substitution of the temperature dependent relationships for the free energy of mixing in equations (38) and (39) into equations (1.27) and (1.28) enables the critical mixing temperature and composition for the appearance or disappearance of the two phase region to be calculated. The values obtained are shown below:

$$\text{Critical temperature: } 361.08^{\circ}\text{K} \quad (4.43)$$

$$\text{Critical composition: } 45.42 \text{ mole per cent KI} \quad (4.44)$$

It can be seen that the data obtained at 367°K is at a temperature only 6° from that of the critical temperature.

The ΔH of mixing is calculated using equation (1.7) with the values of the parameters B_h^s and C_h^s shown in equations (38) and (39). The values of the ΔH of mixing obtained at room temperature by Koski³³ from a least squares fit to his data are compared to the calculated values obtained in the present study (see table IV (9)). An experimental accuracy of ± 30 cal./mole is claimed for the data at the equimolar composition. The agreement between the calculated values in the present study and those measured directly is excellent. The numerical values obtained by other workers was not available other than in graphical form³⁴. The values obtained in the present calculation are shown in detail in Appendix VIII as a function of mole fraction.

The value of ΔS of mixing as a function of mole fraction is

TABLE IV (9)

Experimental ΔH^M Obtained by Koski and Calculated in the Present Study

<u>X</u> <u>1</u>	<u>ΔH^M KI-KBr</u>	
	<u>Koski (experimental at room temperature) in cal.</u>	<u>Present (calculated) in cal. exp.-cal.</u>
.1	158.	154. +4.
.2	278.	271. +7.
.3	359.	351. +8.
.4	404.	397. +7.
.5	415.	409. +6.
.6	392.	389. +3.
.7	338.	336. +2.
.8	253.	253. 0.
.9	140.	141. -1.

shown in Appendix VIII. This was calculated using equation (1.6) and the parameters B_s^S and C_s^S shown in expression (38) and (39).

The values of the ΔG of mixing at 298°K, 361°K (the critical mixing temperature) and 400°K are listed in Appendix V as a function of mole fraction. This is plotted in figure 3. These were calculated using equation (1.3) and the free energy parameters derived in this section.

The solvus curve is calculated by solving equations (1.25) and (1.26) using the temperature dependent free energy parameters for the solid phase shown in equations (38) and (39). The numerical values obtained are shown in Appendix IX.

The solidus-liquidus curves can be calculated from equations (28) and (29) if the temperature dependent parameters in the solid and molten liquid phases and the free energy of fusion of the pure components are known. For the change in state represented by (16) and (17), the value for the ΔS° of mixing at the melting point temperatures shown below have been determined³⁵:

		<u>ΔS° of mixing (in cal/°K)</u>	
KBr	1007°K	6.06	(4.45)

KI	954°K	6.02	(4.46)
----	-------	------	--------

The corresponding value for the free energy change is represented by the following:

$$\Delta G_T^O = \Delta S^\circ (T_{m.p.} - T) \quad (4.47)$$

Thus, solving equations (28) and (29) and using the free energy parameters in expressions (34), (35), (38), and (39) and the free energy of fusion of the pure components shown above by equation (47), the liquidus-solidus curves are calculated. This is shown in figure 4 along with experimental data taken from a graph. Appendix X lists the values obtained.

C. NH₄I-KI at 25°C and NH₄I-KI-H₂O at 25°C

The equilibrium between the solid solutions of NH₄I-KI and its saturated aqueous phase has not been studied before. Complete miscibility for this solid-solid system has been shown experimentally.¹⁶ A probable reason for the lack of experimental data for the three component system is the rapid oxidation of NH₄I in water. This is observed by the red color of I₂ seen in concentrated aqueous NH₄I solutions. In the present study, the decomposition of NH₄I to I₂ has been avoided by the addition to the third component water of a hydroxylamine salt and a base in an amount .2% by weight (see section II). The equilibrium constants of interest are the following:

$$K_1 = \frac{(\gamma_{1\pm})^2 m_{I^-} m_{NH_4^+}}{f_1 x_1} \quad (4.48)$$

$$K_2 = \frac{(\gamma_{2\pm})^2 m_{I^-} m_{K^+}}{f_2 x_2} \quad (4.49)$$

As shown in the last section, the value of K₂ in equation (4.49) has been determined. The activity coefficient of NH₄I in a saturated aqueous 2-component solution has been reported.³⁶ f₁ is equal to unity when X₁ is equal to unity. The solubility of pure NH₄I in water has been determined in the present study (see table III 15). The values obtained for K₁ and K₂ are:

$$K_1 = 59.24 \quad (4.50)$$

$$K_2 = 55.94 \quad (4.51)$$

Employing equations (1.37) through (1.39), the following values of the free energy parameters have been obtained:

$$B_g = .400 \quad , \quad (4.52)$$

$$C_g = -.020 \quad . \quad (4.53)$$

Table IV (10) summarizes the experimental data obtained in the present study. Shown are the experimentally determined values of the activity coefficients in the liquid and solid phases. f_1 and f_2 are evaluated by equations (1.15) and (1.16). Also shown in this table is the value of $\log \frac{\gamma_1^2}{\gamma_2}$. This term was assumed to be a constant in obtaining the B_g and C_g values. As will be seen, the experimental data are reproduced within the limits of the experimental accuracy by making this approximation.

Employing equation (1.33) and (1.34) with the approximation discussed above, the mole fraction of dissolved salts in the liquid phase is calculated and compared with the experimental value in Table IV (11). The value of the $\log \frac{\gamma_1^2}{\gamma_2}$ was taken as the average of the experimental values shown in Table IV (10). The agreement between calculated values and experimental values is excellent. (see figure 5).

Shown in Appendix XII are the values of the free energy of mixing found in the present study.

The value of B_g obtained experimentally for the $\text{NH}_4\text{I-KI}$ system at 298°K is smaller than that for any pair of alkali-metal halides. Proceeding with the assumption that the NH_4^+ ion behaves like an alkali-metal ion as to its thermodynamic behavior in solid solutions formation, the small value of B_g is anticipated. The basis for this prediction is now discussed.

TABLE IV (10)

NH₄I-KI-H₂O at 25°CExperimental Values of Activity Coefficients in Aqueous Liquid and Solid Phase(1 = NH₄I, 2 = KI)

	x_1^s	m_1	m_2	γ_1	γ_2	$\log \frac{\gamma_1^2}{\gamma_2}$	f_1	f_2	log D
A	.2040	3.187	6.703	.7037	.8272	-.1404	1.2915	1.0186	.2683
B	.2050	3.184	6.701	.7057	.8271	-.1379	1.2906	1.0188	.2654
C	.3144	4.477	5.836	.6969	.8156	-.1366	1.2039	1.0439	.2234
D	.3167	4.473	5.836	.6994	.8146	-.1325	1.2023	1.0446	.2185
E	.4090	5.496	5.168	.6880	.8027	-.1340	1.1448	1.0741	.1866
F	.4092	5.475	5.140	.6910	.8066	-.1344	1.1447	1.0742	.1870
G	.5035	6.396	4.421	.6881	.8037	-.1350	1.0981	1.1123	.1545
H	.5046	6.403	4.428	.6878	.8019	-.1332	1.0976	1.1128	.1522
I	.6063	7.394	3.700	.6810	.7900	-.1289	1.0593	1.1633	.1130
J	.6067	7.388	3.676	.6824	.7934	-.1308	1.0591	1.1635	.1150
K	.6664	8.021	3.218	.6754	.7862	-.1320	1.0417	1.1979	.0960
L	.6794	8.220	3.111	.6698	.7833	-.1359	1.0383	1.2059	.0957
M	.7651	9.103	2.375	.6652	.7802	-.1386	1.0200	1.2629	.0707
N	.7673	9.097	2.376	.6664	.7771	-.1335	1.0196	1.2645	.0649

TABLE IV (11)

NH₄I-KI-H₂O at 25°C

Experimental and Calculated Mole Fractions of Dissolved NH₄I
in Aqueous Liquid Phase

	X_1^g	X_1^l Experimental	X_1^l Calculated	Experimental minus Calculated
A	.2040	.3222	.3193	+0.0029
B	.2050	.3221	.3204	+0.0017
C	.3144	.4341	.4329	+0.0012
D	.3167	.4339	.4350	-0.0011
E	.4090	.5154	.5157	-0.0003
F	.4092	.5158	.5158	.0000
G	.5035	.5914	.5910	+0.0004
H	.5046	.5912	.5919	-0.0007
I	.6063	.6664	.6693	-0.0029
J	.6067	.6678	.6696	-0.0018
K	.6664	.7136	.7149	-0.0013
L	.6794	.7254	.7248	+0.0006
M	.7651	.7931	.7915	+0.0016
N	.7673	.7929	.7933	-0.0004

It is found experimentally that the following relationship holds for binary solid solutions of the alkali-metal halides:

$$B_h = \text{constant} \cdot \delta^2$$

$$\text{where } \delta = \frac{a_1 - a_2}{a_1 + a_2} \quad (4.54)$$

For the two systems studied in the present work at 298°K, the values of δ^2 obtained from the data shown in tables III (8) and (14) are shown below:

$$\delta^2 = 11.628 \times 10^{-4} \quad \text{for KI-KBr} \quad (4.55)$$

$$\delta^2 = 1.852 \times 10^{-4} \quad \text{for NH}_4\text{I-KI} \quad (4.56)$$

Solving equation (54) for the KI-KBr system using the value of B_h obtained in equation (38) and the value of δ^2 obtained in equation (55) above, the following value of the constant is obtained:

$$\text{constant} = 7.087 \times 10^5 \quad (4.57)$$

Employing this constant, the value of B_h is obtained for the system $\text{NH}_4\text{I-KI}$ from equations (54) and (56). This is shown below:

$$B_h = 131. \quad (4.58)$$

This is obtained independently of the free energy data obtained in the present study.

The small value of B_h in the $\text{NH}_4\text{I-KI}$ system indicates that the approximation that the series of solid solutions behaves as a strictly regular and symmetrical solution is almost valid. Using this approximation and the value of B_h derived, the value of B_g is obtained:

$$B_g = .44 \quad (\text{calculated using approximations}) \quad (4.59)$$

This value is compared to that calculated from experiment shown in equation (52). Clearly, the values obtained are the same within the limits of error introduced by the approximations involved in deriving equation (59).

Using the approximation of a strictly regular and symmetrical solution, the critical temperature and composition are predicted to be the following:

$$T_c = 60^\circ\text{K} \quad (4.60)$$

$$x_c = .50 \quad (4.61)$$

This critical temperature is valid under conditions where no crystal structure transitions take place in the pure components or in the solid solutions.

D. Conclusions

Phase diagrams, often viewed as "road maps", are of much practical value but as such are of little theoretical interest. In this thesis, the thermodynamic interpretation of phase equilibria has led to most gratifying results. From accurate phase equilibria measurements on the KI-KBr system, the thermodynamic properties of interest in this study have been calculated. Employing only four non-zero parameters to describe both the solid and molten liquid solutions, the calculated properties are shown to reproduce, within the limits of the experimental determinations, the values calculated from experiment for the free energy of mixing over a 1000° range. Further, the calculated properties are shown to be consistent with the experimental data obtained in the present study at 298°K and 367°K, the heats of mixing, and the liquidus-solidus phase equilibria. The experimental confirmation in the $\text{NH}_4\text{I-KI}$ system of the predictions of thermodynamic

properties is very exciting. This suggests the possibility that similar successful predictions can be made for all of the two-component systems of the alkali-metal halides.

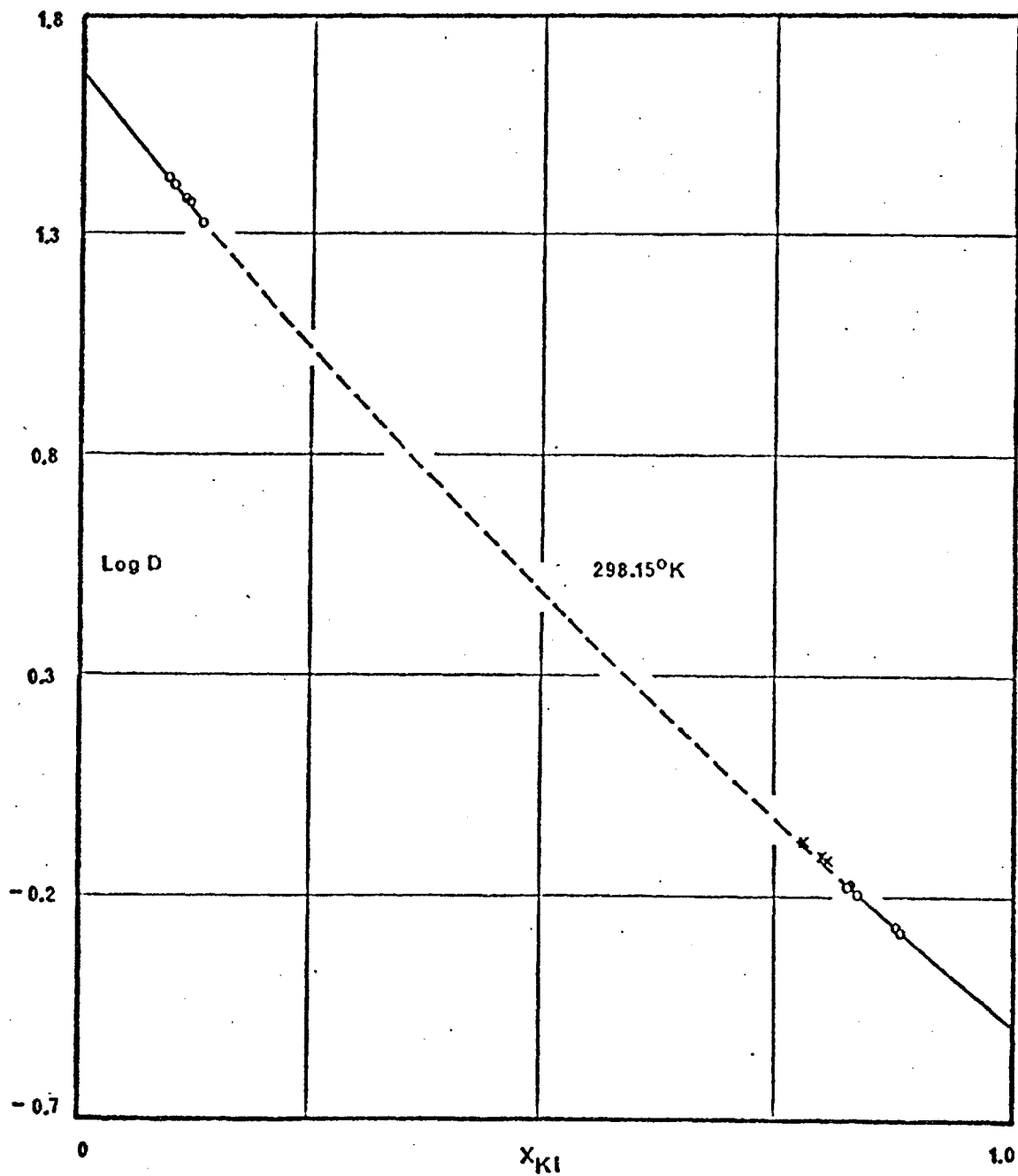


FIGURE 1

KI-KBR-H₂O AT 298.15°K

STABLE: EXPERIMENTAL \circ , CALCULATED (—)
 METASTABLE: EXPERIMENTAL \times , CALCULATED (—)

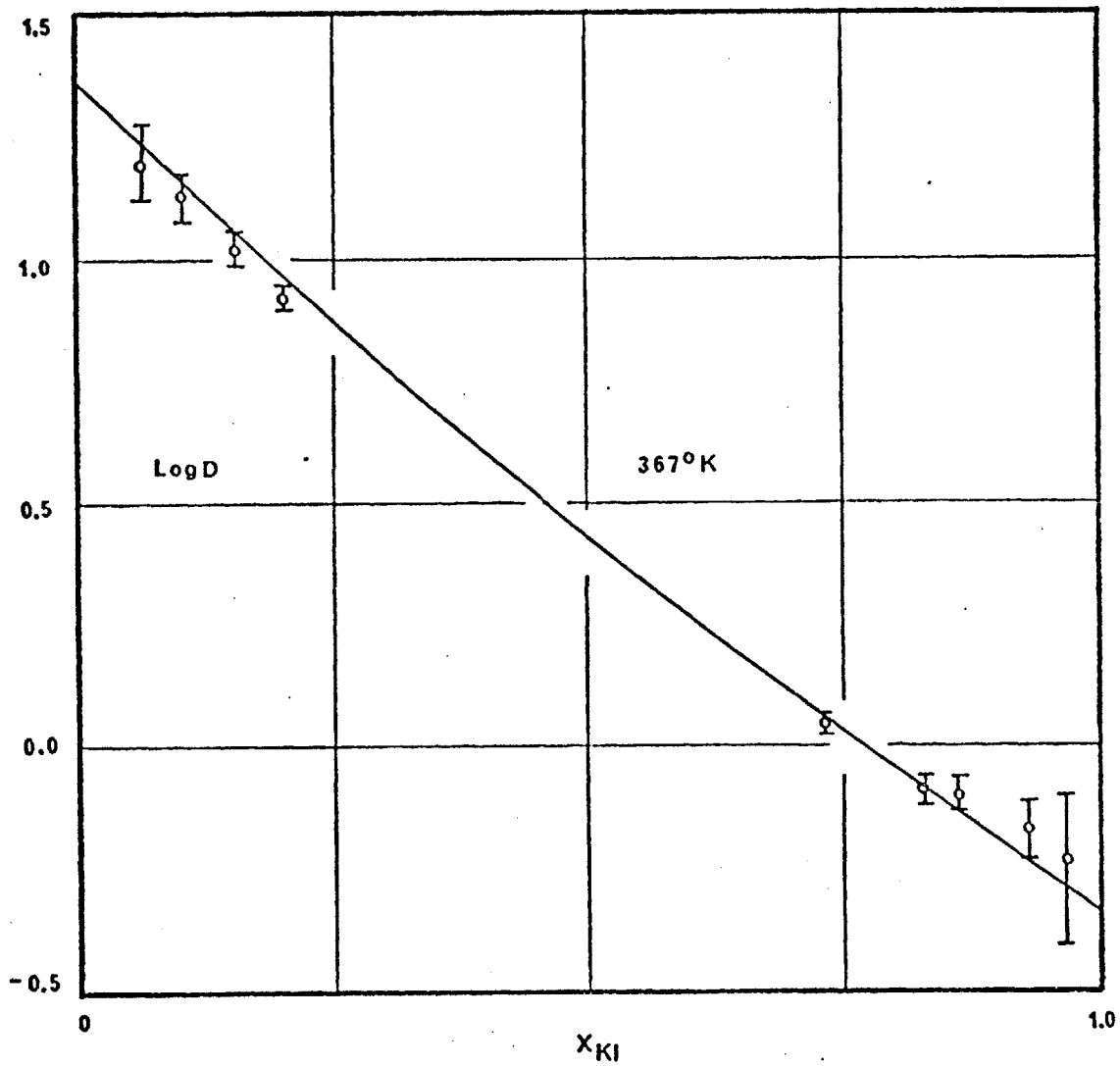


FIGURE 2
 KI-KBR- H_2O AT 367°K
 EXPERIMENTAL \circ , CALCULATED (—)

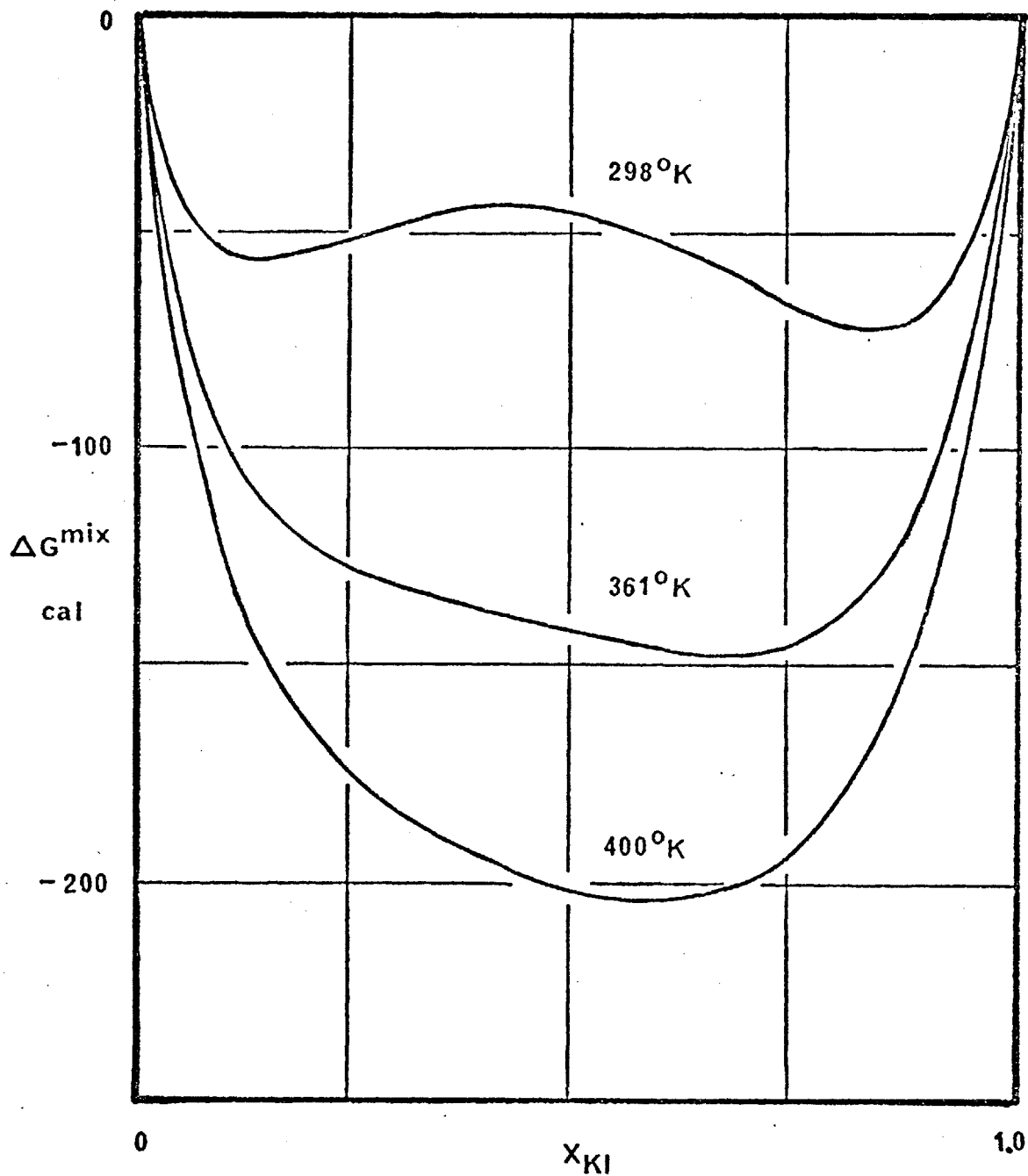


FIGURE 3

FREE ENERGY OF MIXING OF SOLID SOLUTIONS OF KI-KBR
 BELOW THE CRITICAL MIXING TEMPERATURE, AT THE CRITICAL
 MIXING TEMPERATURE, AND ABOVE THE CRITICAL MIXING TEMPERATURE

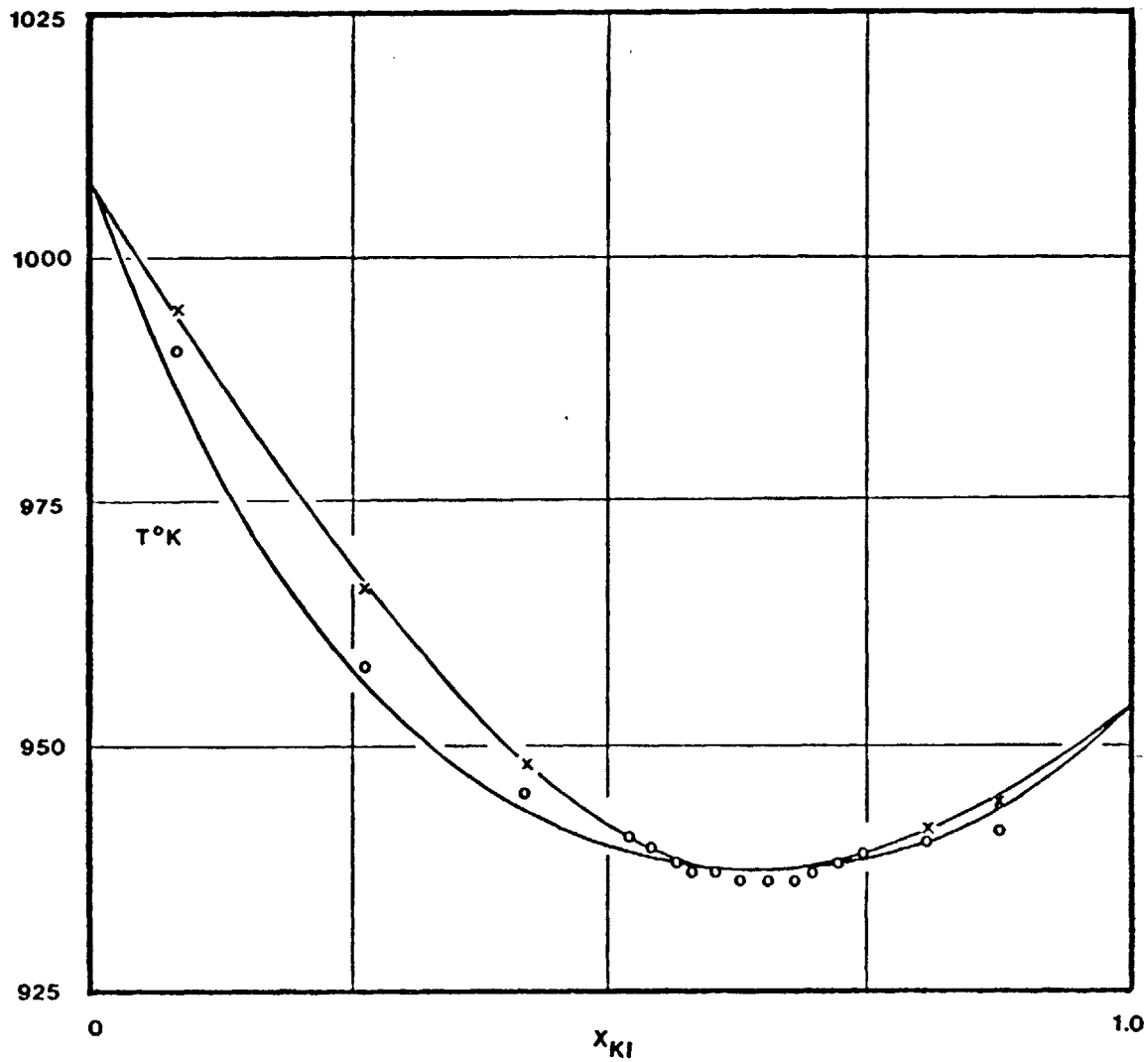


FIGURE 4
 KI-KBR, LIQUIDUS AND SOLIDUS CURVES,
 CALCULATED (—) AND
 (LUOVA AND MUURINEN³¹)

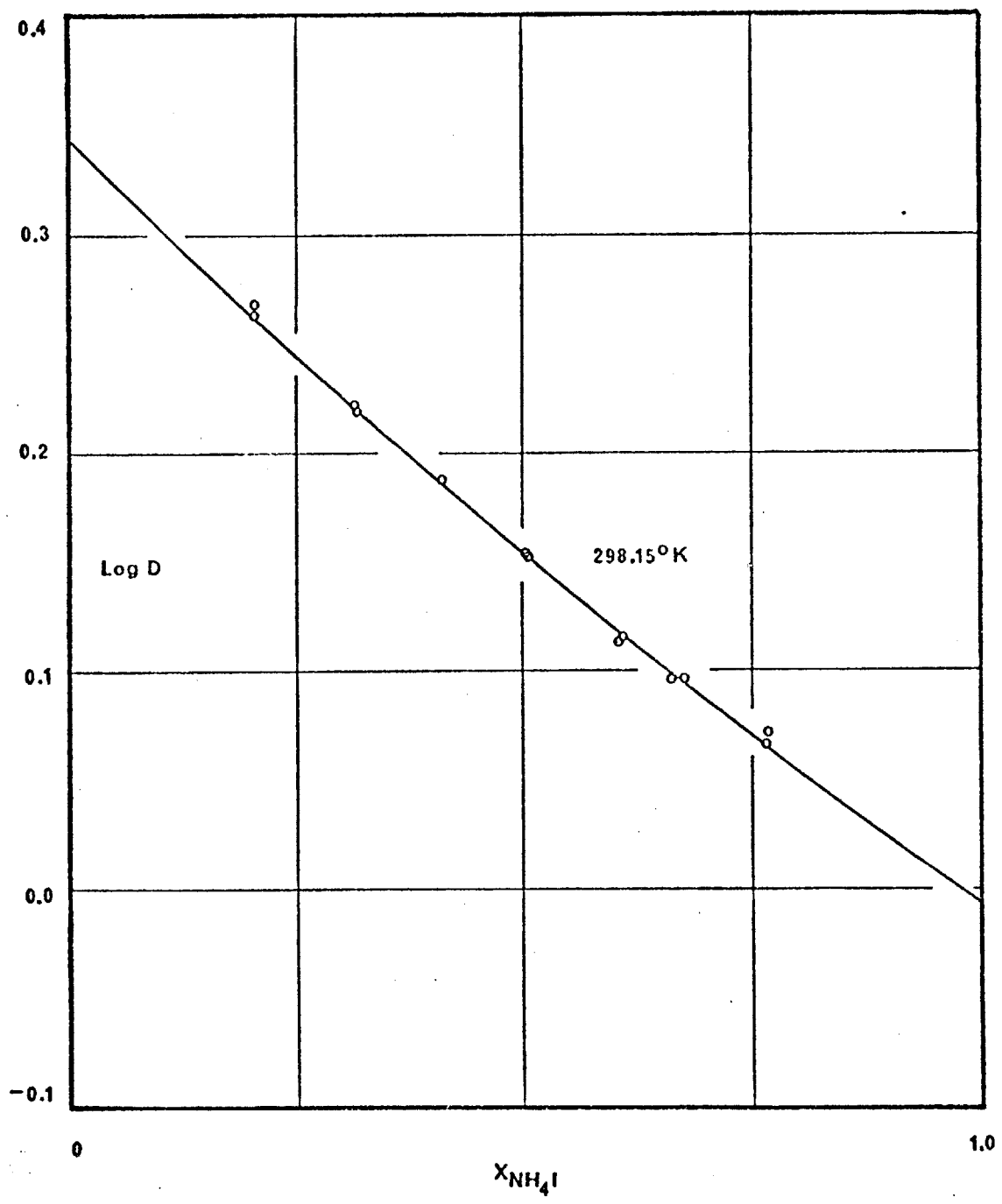


FIGURE 5
NH₄I-KI-H₂O AT 298.15°K
EXPERIMENTAL O, CALCULATED (—)

APPENDIX I

Approximations for the Strictly Regular and Symmetrical Solution

"Strictly regular solutions" are defined as having an ideal entropy of mixing and ΔS^{XS} of zero. "Symmetrical solutions" are those defined as having an excess free energy of mixing symmetrical around $X = .5$. Thus, for a solution which is both strictly regular and symmetrical, $B_g = B_h/T$ and $B_s = 0, C_g = 0, C_s = 0, C_h = 0$. The thermodynamic properties of interest of such a solution are shown below:

$$\Delta G^{XS} = B_h R X_1 X_2 \quad , \quad (A1.1)$$

$$\Delta H^M = B_h R X_1 X_2 \quad , \quad (A1.2)$$

$$\Delta S^{XS} = 0 \quad . \quad (A1.3)$$

At the critical temperature, substitution of $X = .5$ into equation (1.27) yields the following:

$$B_h = 2T_c \quad , \quad B_g = 2 \quad , \quad (A1.4)$$

$$\Delta H(X = .5) = \frac{1}{2} RT_c \quad . \quad (A1.5)$$

APPENDIX II

X-ray Data for Pure Components and Solid Solutions of

KI-KBr and $\text{NH}_4\text{I-KI}$

Pure KI

$a = 7.066 \text{ \AA}$

Film Radius = 5.7200 cm.

<u>Line</u>	<u>θ</u>	<u>$f(\theta)$</u>	<u>$d, \text{ \AA}$</u>	<u>λ</u>
820 α_1	64.08	.191	.8564	7.0620
820 α_2	64.39	.187	.8563	7.0612
822 α_1	67.71	.139	.8325	7.0640
751 α_1	71.89	.089	.8157	7.0642
555 α_1	77.17	.043	.8104	7.0649

Pure KBr

$a = 6.600 \text{ \AA}$

Film Radius = 5.7301 cm.

<u>Line</u>	<u>θ</u>	<u>$f(\theta)$</u>	<u>$d, \text{\AA}$</u>	<u>$a, \text{\AA}$</u>
640 α_1	57.44	.317	.9139	6.5902
642 α_1	60.95	.245	.8811	6.5935
642 α_2	61.22	.241	.8810	6.5928
820 α_1	74.30	.066	.8001	6.5978
820 α_2	74.79	.062	.8002	6.5986
822 α_1	82.03	.017	.7778	6.5999

Pure NH₄I
a=7.261Å

Film Radius = 5.7250 cm.

<u>Line</u>	<u>θ</u>	<u>f(θ)</u>	<u>d, Å</u>	<u>a, Å</u>
731α ₁	54.66	.379	.9442	7.2525
820α ₁	61.11	.243	.8797	7.2542
822α ₁	64.27	.188	.8551	7.2558
911α ₁	75.18	.059	.7968	7.2592
842α ₁	76.49	.048	.7922	7.2606

NH₄I-KI

50.46 Mole per cent NH₄I

Film Radius = 5.7329 cm.

a=7.168Å

<u>Line</u>	<u>θ</u>	<u>f(θ)</u>	<u>d, Å</u>	<u>a, Å</u>
422	31.92	1.329	1.4568	7.1369
511	34.07	1.188	1.3751	7.1453
440	37.58	.993	1.2631	7.1452
531	39.63	.895	1.2077	7.1449
600	40.31	.863	1.1905	7.1430
711	50.27	.498	1.0015	7.1521
640	50.91	.480	.9924	7.1563
642	53.68	.404	.9559	7.1533
731	55.77	.353	.9316	7.1557
820α ₁	62.49	.218	.8685	7.1618

NH₄I-KI

50.35 Mole per cent NH₄I

a=7.168Å

Film Radius = 5.7218 cm.

<u>Line</u>	<u>θ</u>	<u>f(θ)</u>	<u>d, Å</u>	<u>a, Å</u>
422	31.89	1.329	1.4590	7.1476
440	37.59	.993	1.2637	7.1486
600	40.29	.863	1.1921	7.1526
711	50.30	.498	1.0020	7.1557
820α ₁	62.45	.218	.8688	7.1643
822α ₁	65.82	.165	.8444	7.1650
911α ₁	78.35	.036	.7864	7.1644
842α ₁	80.14	.026	.7818	7.1653

KI-KBr

88.6 Mole per cent KI

$a=7.016 \text{ \AA}$

Complex B

Film Radius = 5.7266 cm.

<u>Line</u>	<u>θ</u>	<u>$f(\theta)$</u>	<u>$d, \text{\AA}$</u>	<u>$a, \text{\AA}$</u>
422	32.68	1.276	1.4277	6.9943
511	34.96	1.134	1.3455	6.9915
440	38.52	.948	1.2378	7.0021
531	40.66	.845	1.1831	6.9999
622	46.92	.605	1.0555	7.0013
820 α_1	64.91	.179	.8505	7.0134
822 α_1	68.75	.126	.8264	7.0123

KI-KBr

88.0 Mole per cent KI

$a=7.016 \text{ \AA}$

Complex C

Film Radius = 5.7240 cm.

<u>Line</u>	<u>θ</u>	<u>$f(\theta)$</u>	<u>$d, \text{\AA}$</u>	<u>$a, \text{\AA}$</u>
422	32.69	1.276	1.4271	6.9914
531	40.68	.845	1.1828	6.9976
600	41.34	.819	1.1670	7.0020
711	51.76	.455	.9814	7.0086
640	52.49	.436	.9718	7.0077
642	55.42	.363	.9364	7.0074

KI-KBr

83.7 Mole per cent KI

$a=6.993\text{\AA}$

Complex D

Film Radius = 5.7272 cm.

<u>Line</u>	<u>θ</u>	<u>$f(\theta)$</u>	<u>$d, \text{\AA}$</u>	<u>$a, \text{\AA}$</u>
422	32.75	1.269	1.4250	6.9811
511	35.01	1.134	1.3435	6.9811
440	38.62	.943	1.2352	6.9874
531	40.73	.845	1.1814	6.9893
622	47.05	.602	1.0533	6.9867
640	52.67	.430	.9694	6.9904
642	55.61	.358	.9342	6.9909
731	57.90	.306	.9100	6.9898

KI-KBr

82.8 Mole per cent KI

$a = 6.988\text{\AA}$

Complex E

Film Radius = 5.7272 cm.

<u>Line</u>	<u>θ</u>	<u>$f(\theta)$</u>	<u>$d, \text{\AA}$</u>	<u>$a, \text{\AA}$</u>
422	32.80	1.269	1.4231	6.9718
511	35.06	1.128	1.3418	6.9723
440	38.70	.938	1.2328	6.9738
531	40.83	.841	1.1791	6.9757
622	47.14	.598	1.0517	6.9761
642	55.70	.356	.9332	6.9834
820	65.47	.170	.8474	6.9878

KI-KBr

82.5 Mole per cent KI

$a=6.986\text{\AA}$

Complex F

Film Radius = 5.7275 cm.

<u>Line</u>	<u>θ</u>	<u>$f(\theta)$</u>	<u>$d, \text{\AA}$</u>	<u>$a, \text{\AA}$</u>
422	32.76	1.269	1.4246	6.9791
511	35.02	1.134	1.3432	6.9795
440	38.65	.938	1.2343	6.9823
622	47.11	.598	1.0522	6.9795
711	52.04	.449	.9778	6.9829
640	52.77	.428	.9681	6.9811
642	55.66	.356	.9336	6.9864
731	57.96	.304	.9094	6.9852
820	65.55	.168	.8468	6.9829

KI-KBr

82.1 Mole per cent KI

$a=6.985 \text{ \AA}$

Complex G

Film Radius = 5.7291 cm.

<u>Line</u>	<u>θ</u>	<u>$f(\theta)$</u>	<u>$d, \text{\AA}$</u>	<u>$a, \text{\AA}$</u>
422	32.85	1.263	1.4210	6.9615
511	35.12	1.128	1.3402	6.9639
440	38.76	.933	1.2315	6.9665
531	40.88	.837	1.1779	6.9686
600	41.60	.806	1.1610	6.9660
622	47.13	.598	1.0518	6.9768
711	52.10	.447	.9770	6.9771
640	52.82	.428	.9676	6.9775
642	55.76	.353	.9325	6.9782
731	58.05	.304	.9086	6.9790

KI-KBr

81.6 Mole per cent KI

$a=6.986\text{\AA}$

Complex H

Film Radius = 5.7208 cm.

<u>Line</u>	<u>θ</u>	<u>$f(\theta)$</u>	<u>$d, \text{\AA}$</u>	<u>$a, \text{\AA}$</u>
422	32.84	1.269	1.4215	6.9639
511	35.12	1.128	1.3402	6.9639
440	38.72	.938	1.2323	6.9710
531	40.84	.841	1.1788	6.9739
600	41.54	.810	1.1625	6.9750
622	47.17	.595	1.0512	6.9728
711	52.05	.447	.9775	6.9807
640	52.80	.428	.9677	6.9782
642	55.75	.356	.9327	6.9797
820	65.52	.170	.8470	6.9845

KI-KBr

80.2 Mole per cent KI

$\lambda = 6.974 \text{ \AA}$

Complex I

Film Radius = 5.7250 cm.

<u>Line</u>	<u>θ</u>	<u>$f(\theta)$</u>	<u>$d, \text{ \AA}$</u>	<u>$a, \text{ \AA}$</u>
422	32.88	1.263	1.4202	6.9576
511	35.12	1.128	1.3402	6.9639
440	38.79	.933	1.2304	6.9602
531	40.87	.837	1.1781	6.9698
600	41.61	.806	1.1609	6.9654
622	47.23	.595	1.0501	6.9655
640	52.88	.425	.9667	6.9710
642	55.84	.353	.9317	6.9722
820	65.71	.167	.8458	6.9746

KI-KBr

79.8 Mole per cent KI

$a=6.976 \text{ \AA}$

Complex K

Film Radius - 5.7272 cm.

<u>Line</u>	<u>θ</u>	<u>$f(\theta)$</u>	<u>$d, \text{\AA}$</u>	<u>$a, \text{\AA}$</u>
422	32.90	1.263	1.4192	6.9527
511	35.18	1.123	1.3382	6.9535
440	38.79	.933	1.2305	6.9608
600	41.67	.802	1.1596	6.9576
622	47.23	.595	1.0501	6.9655
640	52.97	.423	.9656	6.9630
642	55.87	.351	.9312	6.9684
731	58.11	.302	.9079	6.9737

KI-KBr

80.1 Mole per cent KI

$a=6.984\text{\AA}$

Complex L

Film Radius = 5.7243 cm.

<u>Line</u>	<u>θ</u>	<u>$f(\theta)$</u>	<u>$d, \text{\AA}$</u>	<u>$a, \text{\AA}$</u>
422	32.86	1.263	1.4210	6.9615
511	35.11	1.128	1.3405	6.9655
440	38.76	.933	1.2313	6.9653
531	40.90	.837	1.1774	6.9656
600	41.63	.806	1.1605	6.9630
711	52.10	.447	.9769	6.9764
640	52.78	.428	.9681	6.9811
731	58.07	.302	.9083	6.9767
820	65.60	.168	.8465	6.9804

KI-KBr

77.8 Mole per cent KI

$a=6.968\text{\AA}$

Complex M

Film Radius = 5.7234 cm.

<u>Line</u>	<u>θ</u>	<u>$f(\theta)$</u>	<u>$d, \text{\AA}$</u>	<u>$a, \text{\AA}$</u>
422	32.96	1.256	1.4158	6.9360
511	35.23	1.123	1.3354	6.9390
440	38.84	.933	1.2282	6.9478
531	40.98	.832	1.1745	6.9485
600	41.72	.802	1.1574	6.9444
622	47.35	.588	1.0480	6.9516
640	53.06	.420	.9645	6.9551
642	56.00	.349	.9299	6.9587
731	58.27	.298	.9064	6.9621
820	65.90	.164	.8445	6.9639

KI-KBr

44.6 Mole per cent KI

a=6.987, 6.663Å

Complex N

Film Radius = 5.7304

α-PHASE

<u>Line</u>	<u>θ</u>	<u>f(θ)</u>	<u>d, Å</u>	<u>a, Å</u>
420	31.26	1.371	1.4856	6.6438
422	34.62	1.158	1.3569	6.6475
622	50.22	.501	1.0031	6.6538
642	60.01	.264	.8901	6.6609

β-PHASE

422	32.82	1.269	1.4223	6.9678
511	35.12	1.128	1.3400	6.9629
440	38.73	.938	1.2321	6.9699
622	47.17	.595	1.0512	6.9728
640	52.84	.428	.9672	6.9746
642	55.72	.356	.9330	6.9819
731	58.02	.304	.9089	6.9814
820	65.57	.168	.8467	6.9821

KI-KBr

12.8 Mole per cent KI

$a=6.657\text{\AA}$

Complex O

Film Radius = 5.7250 cm.

<u>Line</u>	<u>θ</u>	<u>$f(\theta)$</u>	<u>$d, \text{\AA}$</u>	<u>$a, \text{\AA}$</u>
331	30.41	1.436	1.5229	6.6382
420	31.30	1.371	1.4839	6.6361
422	34.68	1.152	1.3548	6.6372
511	37.12	1.019	1.2774	6.6376
440	41.06	.828	1.1736	6.6389
531	43.35	.737	1.1231	6.6444
600	44.15	.706	1.1068	6.6408
620	47.20	.595	1.0506	6.6446
622	50.26	.498	1.0026	6.6504
640	56.76	.330	.9217	6.6465
642	60.14	.262	.8889	6.6519

KI-KBr

11.6 Mole per cent KI

$a=6.651\text{\AA}$

Complex P

Film Radius 5.7234 cm.

<u>Line</u>	<u>θ</u>	<u>$f(\theta)$</u>	<u>$d, \text{\AA}$</u>	<u>$a, \text{\AA}$</u>
331	30.46	1.429	1.5207	6.6286
420	31.33	1.371	1.4824	6.6294
422	34.71	1.152	1.3538	6.6323
511	37.12	1.019	1.2775	6.6381
440	41.07	.828	1.1734	6.6378
620	47.22	.595	1.0504	6.6434
622	50.33	.498	1.0015	6.6431
640	56.76	.330	.9216	6.6457
642	60.28	.258	.8877	6.6429

KI-KBr

10.8 Mole per cent KI

$a=6.648\text{\AA}$

Complex Q

Film Radius = 5.7202 cm.

<u>Line</u>	<u>θ</u>	<u>$f(\theta)$</u>	<u>$d, \text{\AA}$</u>	<u>$a, \text{\AA}$</u>
331	30.49	1.429	1.5196	6.6238
420	31.35	1.364	1.4817	6.6263
422	34.72	1.152	1.3535	6.6308
440	41.10	.828	1.1726	6.6333
620	47.28	.591	1.0493	6.6364
622	50.36	.495	1.0011	6.6405
640	56.80	.330	.9213	6.6436
642	60.25	.258	.8879	6.6444

KI-KBr

10.8 Mole per cent KI

$a=6.650\text{\AA}$

Complex R

Film Radius = 5.7221 cm.

<u>Line</u>	<u>θ</u>	<u>$f(\theta)$</u>	<u>$d, \text{\AA}$</u>	<u>$a, \text{\AA}$</u>
331	30.45	1.429	1.5209	6.6295
420	31.32	1.371	1.4832	6.6330
422	34.68	1.152	1.3547	6.6367
511	37.14	1.019	1.2770	6.6355
440	41.07	.828	1.1735	6.6384
622	50.32	.498	1.0016	6.6438
640	56.83	.330	.9210	6.6414
642	60.24	.260	.8881	6.6459

KI-KBr

Complex S

9.4 Mole per cent KI

Film Radius = 5.7240 cm.

$a=6.642\text{\AA}$

<u>Line</u>	<u>θ</u>	<u>$f(\theta)$</u>	<u>$d, \text{\AA}$</u>	<u>$a, \text{\AA}$</u>
420	31.36	1.364	1.4815	6.6254
422	34.71	1.152	1.3538	6.6323
511	37.14	1.019	1.2770	6.6355
440	41.11	.828	1.1724	6.6321
620	47.33	.591	1.0484	6.6307
622	50.40	.495	1.0005	6.6365
642	60.37	.256	.8869	6.6369

KI-KBr

Complex T

9.0 Mole per cent KI

Film Radius = 5.7240 cm.

$a=6.644\text{\AA}$

<u>Line</u>	<u>θ</u>	<u>$f(\theta)$</u>	<u>$d, \text{\AA}$</u>	<u>$a, \text{\AA}$</u>
422	34.80	1.146	1.3509	6.6181
511	37.26	1.008	1.2733	6.6163
440	41.18	.823	1.1709	6.6237
620	47.41	.588	1.0471	6.6225
622	50.46	.492	.9996	6.6305
640	60.41	.256	.8865	6.6339

APPENDIX III

KI-KBr-H₂O at 25°C

Calculated using $\log \frac{\gamma_1^2}{\gamma_2} =$ function of m_1 and m_2 employing equations (4.11) and (4.12)

Valid only in range of experimental data for total molalities.

x_1^s	m_1	m_2	γ_1	γ_2	x_1^l	m_T	Weight % Salts	log D
.10	6.856	2.481	.8319	.7325	.7343	9.337	58.91	1.3957
.15	7.557	2.193	.8401	.7540	.7751	9.750	60.25	1.2907
.20	7.826	2.082	.8439	.7630	.7899	9.908	60.74	1.1772
.21	7.850	2.071	.8443	.7638	.7912	9.922	60.78	1.1540
.25	7.884	2.057	.8448	.7650	.7931	9.941	60.84	1.0607
.30	7.833	2.081	.8441	.7633	.7901	9.914	60.75	.9437
.35	7.726	2.134	.8425	.7599	.7835	9.860	60.58	.8275
.40	7.594	2.206	.8407	.7559	.7749	9.800	60.37	.7129
.45	7.458	2.288	.8390	.7521	.7653	9.745	60.16	.6004
.50	7.330	2.371	.8375	.7489	.7556	9.702	59.99	.4902
.55	7.223	2.450	.8363	.7463	.7467	9.673	59.85	.3824
.60	7.142	2.515	.8354	.7446	.7396	9.657	59.76	.2772
.65	7.096	2.556	.8349	.7438	.7352	9.652	59.71	.1746
.70	7.091	2.561	.8349	.7437	.7347	9.652	59.71	.0744
.75	7.135	2.511	.8353	.7443	.7397	9.647	59.73	-.0236

(continued on following page)

APPENDIX III (cont.)

X_1^s	m_1	m_2	γ_1	γ_2	X_1^l	m_T	Weight % Salts	log D
.79	7.214	2.417	.8361	.7452	.7490	9.631	59.76	-.1005
.80	7.240	2.384	.8363	.7455	.7523	9.624	59.77	-.1195
.85	7.424	2.141	.8378	.7472	.7762	9.566	59.80	-.2133
.90	7.720	1.729	.8394	.7497	.8171	9.449	59.80	-.3043
.95	8.193	1.058	.8395	.7542	.8857	9.250	59.77	-.3897

APPENDIX IV

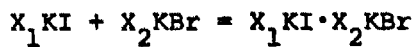
KI-KBr-H₂O at 298.15°K

Calculated for Whole Range of Mole Fractions in Aqueous

Liquid Phase and Solid Phase Assuming $\log \frac{\gamma_1^2}{\gamma_2} = \text{Constant}$

X_1^s	X_1^l	log D
.0001	.0045	1.6538
.0100	.3005	1.6288
.0500	.6399	1.5284
.1000	.7383	1.4048
.1500	.7720	1.2830
.2000	.7845	1.1633
.2100	.7857	1.1396
.2500	.7873	1.0455
.3000	.7847	.9297
.3500	.7789	.8158
.4000	.7712	.7039
.4500	.7626	.5939
.5000	.7538	.4859
.5500	.7456	.3799
.6000	.7390	.2758
.6500	.7348	.1737
.7000	.7343	.0736
.7500	.7392	-.0246
.7900	.7485	-.1018
.8000	.7518	-.1209
.8500	.7754	-.2151
.9000	.8160	-.3074
.9500	.8838	-.3978
.9900	.9711	-.4687
.9999	.9997	-.4860

APPENDIX V



Free Energy of Mixing for the KI·KBr System at
298.15°K, 361.08°K (the critical temperature) and at 400.00°K

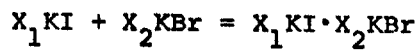
X_1	$\Delta G_{298.15^\circ\text{K}}^{\text{M}}$ (calories)	$\Delta G_{361.08^\circ\text{K}}^{\text{M}}$ (calories)	$\Delta G_{400.00^\circ\text{K}}^{\text{M}}$ (calories)
0	0	0	0
.05	-44.45	-71.05	-87.51
.10	-54.77	-98.79	-126.02
.15	-56.32	-113.95	-149.60
.20	-54.29	-122.86	-165.27
.25	-51.03	-128.38	-176.21
.30	-47.80	-132.06	-184.17
.35	-45.33	-134.81	-190.16
.40	-44.03	-137.18	-194.79
.45	-44.11	-139.44	-198.39
.50	-45.64	-141.68	-201.08
.55	-48.53	-143.85	-202.81
.60	-52.59	-145.74	-203.35
.65	-57.50	-146.98	-202.33
.70	-62.78	-147.04	-199.15
.75	-67.75	-145.10	-192.93
.80	-71.41	-139.98	-182.39
.85	-72.24	-129.87	-165.52
.90	-67.61	-111.63	-138.86
.95	-52.07	-78.68	-95.13
1.00	0	0	0

APPENDIX VI

Activities of KI and KBr in Solid Phase at 298°K

X_1	a_1	a_2	1 = KI 2 = KBr
0	.0000	1.0000	
.05	.5154	.9569	
.10	.7920	.9261	
.15	.9296	.9058	
.20	.9872	.8947	
.25	1.0000	.8915	
.30	.9889	.8954	
.35	.9666	.9054	
.40	.9403	.9205	
.45	.9145	.9397	
.50	.8917	.9614	
.55	.8734	.9836	
.60	.8605	1.0034	
.65	.8535	1.0170	
.70	.8528	1.0185	
.75	.8586	1.0000	
.80	.8713	.9499	
.85	.8912	.8521	
.90	.9188	.6842	
.95	.9549	.4147	
1.00	1.0000	0000	

APPENDIX VII



T = 367°K

Calculated Mole Fractions Dissolved Salts in Aqueous
Phase and Solid Phase

X_1^s	X_1^l	log D
.0001	.0023	1.3572
.0100	.1801	1.3374
.0500	.4880	1.2578
.1000	.6162	1.1598
.1500	.6713	1.0635
.2000	.6993	.9687
.2100	.7031	.9499
.2500	.7145	.8754
.3000	.7226	.7838
.3500	.7268	.6938
.4000	.7288	.6054
.4500	.7297	.5185
.5000	.7306	.4333
.5500	.7322	.3496
.6000	.7353	.2675
.6500	.7407	.1871
.7000	.7496	.1082
.7500	.7631	.0309
.7900	.7784	-.0298
.8000	.7830	-.0448
.8500	.8117	-.1189
.9000	.8528	-.1914
.9500	.9122	-.2624
.9900	.9794	-.3179
.9999	.9998	-.3316

APPENDIX VIII

ΔH^M and ΔS^M Calculated

<u>X_1</u>	<u>ΔH^M Calculated (cal)</u>	<u>ΔS^M Calculated (cal/°K mole)</u>
.0	0	0
.05	81.60	.4228
.10	153.80	.6996
.15	216.75	.9159
.20	270.58	1.0896
.25	315.41	1.2291
.30	351.39	1.3389
.35	378.64	1.4220
.40	397.31	1.4803
.45	407.52	1.5148
.50	409.40	1.5262
.55	403.10	1.5148
.60	388.75	1.4803
.65	366.47	1.4220
.70	336.41	1.3389
.75	298.69	1.2291
.80	253.46	1.0896
.85	200.84	.9159
.90	140.97	.6996
.95	73.98	.4228
1.00	0	0

APPENDIX IX

Calculated Solvus Curve

<u>KI-KBr</u>	<u>Mole Fraction KI</u>	
<u>T°K</u>	<u>α</u>	<u>β</u>
273.15	.0854	.8761
283.15	.1004	.8564
293.15	.1175	.8342
298.15	.1270	.8220
303.15	.1372	.8090
313.15	.1603	.7803
323.15	.1875	.7470
333.15	.2206	.7075
344.15	.2679	.6527
346.15	.2784	.6408
348.15	.2898	.6280
350.15	.3024	.6140
352.15	.3162	.5987
354.15	.3320	.5815
356.15	.3505	.5615
358.15	.3738	.5368

Critical Point:

361.08	45.42	45.42
--------	-------	-------

APPENDIX X

Liquidus-solidus curves calculated

x_1^s	<u>KI-KBr</u> x_1	$T^\circ K$
.0500	.0893	992.87
.1000	.1651	981.25
.1500	.2302	971.73
.2000	.2870	963.93
.2500	.3372	957.55
.3000	.3827	952.35
.3500	.4245	948.12
.4000	.4638	944.73
.4500	.5014	942.05
.5000	.5382	940.02
.5500	.5749	938.58
.6000	.6120	937.72
.6500	.6501	937.43
.7000	.6900	937.71
.7500	.7322	938.61
.8000	.7772	940.16
.8500	.8259	942.41
.9000	.8787	945.43
.9500	.9366	949.27

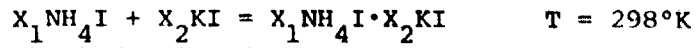
APPENDIX XI

$$X_1 \text{NH}_4\text{I} + X_2 \text{KI} = X_1^g \text{NH}_4\text{I} + X_2^g \text{KI} \quad T = 298^\circ\text{K}$$

Mole Fraction X_1^g and X_1^l Calculated

X_1^g	X_1^l	log D
.0001	.0002	.3417
.0100	.0215	.3378
.0500	.0995	.3219
.1000	.1823	.3023
.1500	.2530	.2830
.2000	.3146	.2640
.2100	.3261	.2602
.2500	.3696	.2452
.3000	.4193	.2266
.3500	.4652	.2083
.4000	.5082	.1903
.4500	.5490	.1726
.5000	.5883	.1551
.5500	.6267	.1378
.6000	.6646	.1208
.6500	.7024	.1041
.7000	.7406	.0877
.7500	.7796	.0715
.7900	.8115	.0587
.8000	.8197	.0555
.8500	.8613	.0399
.9000	.9050	.0244
.9500	.9510	.0093
.9900	.9899	-.0026
.9999	.9999	-.0056

APPENDIX XII



Free Energy of Mixing

X_1	ΔG^{ID} calories	ΔG^{XS} calories	ΔG^{M} calories
.0001	-0.60	.02	-0.58
.0100	-33.18	2.46	-30.72
.0500	-117.62	11.76	-105.85
.1000	-192.61	22.18	-170.42
.1500	-250.45	31.27	-219.17
.2000	-296.48	39.06	-257.42
.2500	-333.17	45.55	-287.63
.3000	-361.93	50.76	-311.16
.3500	-383.60	54.72	-328.88
.4000	-398.75	57.45	-341.30
.4500	-407.71	58.95	-348.76
.5000	-410.68	59.25	-351.43
.5500	-407.71	58.36	-349.35
.6000	-398.75	56.31	-342.44
.6500	-383.60	53.11	-330.49
.7000	-361.93	48.77	-313.15
.7500	-333.17	43.33	-289.85
.8000	-296.48	36.78	-259.70
.8500	-250.45	29.16	-221.29
.9000	-192.61	20.48	-172.13
.9500	-117.62	10.75	-106.87
.9900	-33.18	2.23	-30.95
.9999	-0.60	0.02	-0.58

REFERENCES

1. J. A. Beattie, Introduction to Chemical Thermodynamics.
2. G. Scatchard and W. J. Hamer, *J. Amer. Chem. Soc.* 57, 1805-1809 (1935).
3. J. B. Thompson, Jr. and D. R. Waldbaum, *Geochimica et Cosmochimica Acta* 33, 671-690 (1969).
4. L. Erdey (trans. by G. Svehla), Gravimetric Analysis, Macmillan, New York (1963), Parts I and II (especially chapters 49 and 50).
5. L. A. Janders, Thesis. M. I. T., (1952).
6. H. P. Klug and L. E. Alexander, X-ray Diffraction Procedures for Polycrystalline and Amorphous Materials, Wiley, New York (1954).
7. D. P. Shoemaker and C. W. Garland, Experiments in Physical Chemistry, McGraw-Hill, New York (1962), Chap. XIV.
8. W. H. McCoy and W. E. Wallace, *J. Amer. Chem. Soc.* 78, 1830 (1956).
9. L. L. Makarov, K. K. Evstrop'ev, and Yu. G. Vlasov, *Zhur. Fiz. Khim.* 32, 1618 (1958).
10. H. Lipson and H. Steeple, Interpretation of X-ray Powder Diffraction Patterns, St. Martin's Press, New York (1970), table p316.
11. H. E. Swanson and E. Tatge, *N. B. S. Circular* 539, Vol. I, 66-69 (1953).
12. Asahi Glass Co. (by Narihisa Nishio), *Chem. Abstracts* 68, 5915 (1968), entry 61074c.
13. H. E. Swanson, R. K. Fuyat, and G.M. Urgrinic, *N. B. S. Circular* 539, Vol. IV, 56-57 (1955).
14. M. Amadori and G. Pampanini, *G. Atti R. Acad. Lincei, Rend. Classe Sci. Fis., Mat., Nat.* 5, 20II 478(1911).
15. G. Bruni, *Chem. Rev.* 1, 345 (1925).
16. R. J. Havinghurst, E. Mack and F. C. J. Blake, *J. Amer. Chem. Soc.* 47, 29 (1925).
17. M. Kantola, P. Luova and L. Vinko, *Ann. Acad. Sci. Fenn.* AVI, 164 (1964).
18. P. Luova, *Suomen Kemistilehti* B38, 32 (1965).
19. P. Luova and O. Tannila, *Suomen Kemistilehti* B39, 11 (1966).
20. L. L. Makarov and K. K. Evstrop'ev, *Zh. Fiz. Khim.* 34, 1967 (1960).

21. I. R. Nair and C. T. Walker, *Physical Review B* 7, 6, 2740 (1973).
22. A. Seidell, *Solubilities of Inorganic and Metal Organic Compounds*, 4th edition, Vol. II, Van Nostrand, New York (1965), (Data of Mukimov, Kapkaeva and Bergman, 1952).
23. K. A. Zhdanov, *Doklady Akad. Nauk. Usbek.* 3, 32 (1960).
24. E. Zimmer, Thesis. Lausanne, 1953.
25. R. A. Robinson and R. H. Stokes, *Electrolyte Solutions*, Academic Press, New York, (1959). (Appendix 8.10 especially).
26. J. E. Ricci, *Phase Rule and Heterogeneous Equilibrium*, Van Nostrand, New York (1951).
27. H. S. Harned and R. A. Robinson, *Multicomponent Electrolyte Solutions*, Pergamon Press, Oxford (1968), Pages 84-86.
28. J. Nyvlt, R. Rychly, J. Gottfried and J. Wurzelova, *J. Crystal Growth* 6, 151-62 (1970).
29. J. B. Wrzesnewsky, *Z. Anorg. Chem.* 74,95 (1912).
30. M. Amadori and G. Pampanini, *Atti della Reale Accad. dei Lincei*, 5, 20, II, 572 (1911).
31. P. Luova and M. Muurinen, *Ann. Univ. Turku.* A, 110 (1967).
32. O. J. Kleppa, L. S. Hersh and J. M. Toguri, *Acta Chem. Scandinavica* 17, 2681-2687 (1963).
33. H. Koski, *Suomen Kemistilehti B* 43, 482 (1970).
34. M. W. Lister and N. F. Meyers, *J. Phys. Chem.* 62, 145 (1958).
35. A. S. Dworkin and M. A. Bredig, *J. Phys. Chem.* 64, 269 (1960).
36. M. M. Shul'ts, L. L. Makarov and N. P. Romasheva, *Vestn. Leningrad. Univ. Fiz. Khim.* 4, 78-82 (1971).

BIOGRAPHICAL NOTE

The author is the son of Mr. and Mrs. Abraham Weintraub. He was born in Brooklyn, New York, on October 4, 1949. He attended George W. Wingate High School in Brooklyn, where he received his diploma in January 1967. From February 1967 to January 1971 he attended Hunter College of the City University of New York. He received a Bachelor of Science degree in Chemistry. From February 1971 to the present he has attended the Massachusetts Institute of Technology.